

6-30-2016

# Polyphenols As Natural, Dual-Action Therapeutics For Alzheimer's Disease

Kayla M. Pate

*University of South Carolina*

Follow this and additional works at: <http://scholarcommons.sc.edu/etd>



Part of the [Chemical Engineering Commons](#)

---

## Recommended Citation

Pate, K. M.(2016). *Polyphenols As Natural, Dual-Action Therapeutics For Alzheimer's Disease*. (Doctoral dissertation). Retrieved from <http://scholarcommons.sc.edu/etd/3442>

This Open Access Dissertation is brought to you for free and open access by Scholar Commons. It has been accepted for inclusion in Theses and Dissertations by an authorized administrator of Scholar Commons. For more information, please contact [SCHOLARC@mailbox.sc.edu](mailto:SCHOLARC@mailbox.sc.edu).

**POLYPHENOLS AS NATURAL, DUAL-ACTION THERAPEUTICS FOR ALZHEIMER'S  
DISEASE**

by

**Kayla M. Pate**

**Bachelor of Science  
Auburn University, 2011**

---

Submitted in Partial Fulfillment of the Requirements

For the Degree of Doctor of Philosophy in

**Chemical Engineering**

College of Engineering and Computing

University of South Carolina

2016

Accepted by:

**Melissa A. Moss, Major Professor**

**Esmaiel Jabbari, Committee Member**

**Alexander McDonald, Committee Member**

**Mark Uline, Committee Member**

**John, Weidner, Committee Member**

**Lacy Ford, Senior Vice Provost and Dean of Graduate Studies**

© Copyright by Kayla M. Pate, 2016  
All Rights Reserved.

## ACKNOWLEDGEMENTS

I would like to thank my mother, Debbie, for all of her love, support, and understanding over the years. I truly could not have done this without her. I would also like to thank my family and friends. They may not have always understood what I was talking about, but that never stopped them from listening and offering support. I would like to thank Dr. Will Reed, Dr. Bob Price, and Dr. Shekhar Patel for the training, advice, and mentorship they gave me. I am truly thankful for my cohorts Dr. Katy Rutledge, Dr. Greg Harris, Zebulon Vance, Shelby Chastain, Kendall Murphy, Michael Hendley, and J.C. Rothford who have traveled this road with me, also giving their blood, sweat, and tears for science. They not only offered help with my research but offered friendship, often in the form of happy hours and trivia nights. I would like to thank Dr. Mark Byrne for giving me the opportunity to be involved in research as an undergraduate as well as all the other mentors at Auburn University who gave me the knowledge and support necessary to make it through graduate school. I was also lucky enough to have great friends at Auburn University without whom I would not have made it through my undergraduate program. I will always be thankful for their continued friendship and support. Finally, I would like to thank my professor Dr. Melissa Moss as well as all the previous and current lab members for their help, especially two of my undergraduate research assistances John Clegg and Mac Rogers.

## ABSTRACT

Alzheimer's disease (AD), the most common form of dementia, is characterized by extracellular plaques in the brain created when monomeric amyloid- $\beta$  (A $\beta$ ) protein aggregates into fibrillar structures. Soluble A $\beta$  aggregates, including oligomers, that form along the reaction pathway are believed to be the primary pathogenic species and have been shown to increase the production of reactive oxygen species (ROS). This upregulation of ROS is one suggested contributing factor of A $\beta$  aggregate cytotoxicity and has proven capable of mediating cell signaling associated with A $\beta$  aggregate-induced cellular responses.

Polyphenols have been suggested as a complimentary AD therapeutic based on epidemiological evidence that polyphenol-rich diets correlate with a reduced incidence of AD. Polyphenols have demonstrated the ability to inhibit A $\beta$  aggregation thereby neutralizing the protein's damaging effects. Additionally, polyphenols may counteract A $\beta$  aggregate-induced cellular responses by neutralizing ROS through their antioxidant properties. This study sought to identify polyphenols that can reduce A $\beta$  oligomer-induced cellular responses by 1) altering oligomer formation via changing oligomer size distribution and/or modulating oligomer conformation and 2) exerting antioxidant capabilities. The ability of polyphenols to function as dual-action therapeutics for AD by acting through both mechanisms was also explored.

Many of the studied polyphenols exhibited the ability to alter oligomer formation by both reducing the amount of 25 – 250 kDa oligomers formed and by changing oligomer

surface hydrophobicity. Key polyphenol structural elements were identified that dictate the polyphenol's ability to alter oligomer formation, providing insights into the optimum inhibitor structure. Additionally, these polyphenol-induced changes in A $\beta$  oligomer size distribution and structure resulted in lowered cellular responses, including both intracellular ROS and caspase activation. Polyphenols also exhibited strong antioxidant capabilities, and thus many polyphenols were able to reduce intracellular ROS and caspase activation induced by native A $\beta$  oligomers. These findings demonstrate that polyphenols can attenuate oligomer-induced cellular responses even without altering oligomer formation. Studies also investigated by which mechanism each polyphenol primarily reduces oligomer-induced cellular responses and identified the polyphenol kaempferol as a potential dual-action therapeutic exhibiting synergy between the two mechanisms. Combined, these studies identify several promising polyphenols for use as natural therapeutics for AD.

## TABLE OF CONTENTS

ACKNOWLEDGEMENTS.....	iii
ABSTRACT .....	iv
LIST OF FIGURES .....	ix
LIST OF SYMBOLS .....	xi
LIST OF ABBREVIATIONS.....	xii
CHAPTER 1: BACKGROUND AND SIGNIFICANCE .....	1
1.1 ALZHEIMER'S DISEASE AND THE ROLE OF THE AMYLOID- $\beta$ PROTEIN .....	1
1.2 THE DAMAGING EFFECTS OF A $\beta$ OLIGOMERS.....	3
1.3 ALTERATIONS OF A $\beta$ OLIGOMERS BY POLYPHENOLS AS A THERAPEUTIC APPROACH FOR AD .....	4
1.4 POLYPHENOLS' ANTIOXIDANT CAPABILITIES AS A THERAPEUTIC APPROACH FOR AD .....	5
1.5 STUDY OVERVIEW.....	5
1.6 INNOVATION.....	7
CHAPTER 2: MATERIALS AND METHODS .....	10
2.1 MATERIALS .....	10
2.2 PREPARATION OF A $\beta$ <sub>1-42</sub> OLIGOMERS.....	10
2.3 DETERMINATION OF A $\beta$ <sub>1-42</sub> OLIGOMER SIZE VIA SDS-PAGE AND WESTERN BLOT.....	11
2.4 ASSESSMENT OF A $\beta$ <sub>1-42</sub> OLIGOMER CONFORMATION VIA ANS SPECTROSCOPY .....	12

2.5 ASSESSMENT OF A $\beta$ <sub>1-42</sub> OLIGOMER CONFORMATION VIA NILE RED SPECTROSCOPY .....	13
2.6 DETERMINATION OF POLYPHENOLS' ANTIOXIDANT CAPACITY VIA ORAC ASSAY.....	13
2.7 MEDIA AND CELL LINES.....	14
2.8 ANALYSIS OF POLYPHENOLS' ABILITY TO REDUCE OLIGOMER-INDUCED INTRACELLULAR ROS VIA DCFH-DA ASSAY .....	14
2.9 ANALYSIS OF POLYPHENOLS' ABILITY TO REDUCE OLIGOMER-INDUCED CASPASE ACTIVATION.....	15
2.10 STATISTICAL ANALYSIS.....	17
CHAPTER 3: POLYPHENOLS ATTENUATE A $\beta$ OLIGOMER-INDUCED CELLULAR RESPONSES .....	18
3.1 INTRODUCTION .....	18
3.2 MATERIALS AND METHODS.....	20
3.3 RESULTS .....	22
3.4 DISCUSSION .....	28
CHAPTER 4: QUERCETIN METABOLITES ARE EQUALLY AS EFFECTIVE AS QUERCETIN AT ATTENUATING A $\beta$ OLIGOMER-INDUCED CELLULAR RESPONSES.....	44
4.1 INTRODUCTION .....	44
4.2 MATERIALS AND METHODS.....	46
4.3 RESULTS .....	49
4.4 DISCUSSION .....	54
CHAPTER 5: CONCLUSIONS .....	67
CHAPTER 6: FUTURE PERSPECTIVES .....	71
REFERENCES .....	73
APPENDIX A – MATLAB CODE .....	85

APPENDIX B – EXAMPLE OUTPUT FROM MATLAB CODE .....	92
APPENDIX C – COINCIDING IMAGES FOR FIGURE 3.6.....	93
APPENDIX D – COINCIDING IMAGES FOR FIGURES 4.4 AND 4.5 .....	96

## LIST OF FIGURES

Figure 1.1 The progression of A $\beta$ aggregation .....	9
Figure 3.1 Polyphenol structures .....	34
Figure 3.2 Polyphenols alter A $\beta$ oligomer size distribution .....	35
Figure 3.3 Polyphenols alter A $\beta$ oligomer surface hydrophobicity .....	37
Figure 3.4 A $\beta$ oligomers increase intracellular ROS and caspase activation in human neuroblastoma cells.....	38
Figure 3.5 Polyphenols possess potent antioxidant capability and reduce A $\beta$ oligomer-induced intracellular ROS.....	40
Figure 3.6 Polyphenols reduce A $\beta$ -induced caspase activation .....	42
Figure 4.1 Structure of quercetin metabolites .....	60
Figure 4.2 Quercetin and metabolites possess strong antioxidant capability and reduce A $\beta$ oligomer-induced cellular responses.....	61
Figure 4.3 Quercetin and metabolites alter A $\beta$ oligomer size distribution and conformation .....	63
Figure 4.4 Alterations to A $\beta$ oligomer size distribution and conformation reduce A $\beta$ oligomer-induced cellular responses.....	65
Figure 4.5 Dual-action potential of quercetin and metabolites to reduce A $\beta$ oligomer-induced cellular responses .....	66
Figure B.1 Example output from Matlab code .....	92
Figure C.1 Caspase images for cells treated with A $\beta$ oligomers made in the presence of polyphenol.....	93
Figure C.2 Caspase images for cells treated with A $\beta$ oligomers made in the absence of polyphenol and 40 $\mu$ M polyphenol.....	94
Figure C.3 Caspase images for dual-action treatment .....	95

Figure D.1 Coinciding Hoechst images for Figures 4.4 and 4.5.....96

## LIST OF SYMBOLS

M Molar, abbreviation for SI unit mol / L

p p-value test statistic

## LIST OF ABBREVIATIONS

Aβ.....	amyloid- $\beta$ protein
A $\beta$ <sub>1-40</sub> .....	40 amino acid isoform of amyloid- $\beta$ protein
A $\beta$ <sub>1-42</sub> .....	42 amino acid isoform of amyloid- $\beta$ protein
AD.....	Alzheimer's disease
ANOVA .....	analysis of variance
ANS.....	8-anilino-1-naphthalenesulphonic acid
API.....	apigenin
APP .....	amyloid precursor protein
DCFH.....	2',7' dichlorodihydrofluorescein diacetate
DCFH-DA.....	2', 7'-dichlorodihydrofluorescein
DMSO.....	dimethyl sulfoxide
FLA.....	flavone
HFIP.....	1,1,1,3,3,3-hexafluoro-2-propanol
IAUC.....	integrated area under the curve
IRHA.....	isorhamnetin
KAE .....	kaempferol
LUT.....	luteolin
ORAC .....	oxygen radical absorbance capacity
PRF .....	phenol-red free
QUE .....	quercetin
RHA .....	rhamnetin

ROS.....	reactive oxygen species
TAM.....	tamarixetin

# CHAPTER 1

## BACKGROUND AND SIGNIFICANCE

### **1.1 Alzheimer's Disease and the Role of the Amyloid- $\beta$ Protein**

Alzheimer's disease (AD) is the most common neurodegenerative disease and affects an estimated 5.3 million people in the United States alone.<sup>1</sup> This number is expected to increase as the population of people over the age of 65 continues to grow. While other top leading causes of death such as heart disease, stroke, and HIV have decreased between the years 2000 and 2010, the number of fatalities due to AD has increased 68%.<sup>2</sup> Despite the overwhelming need for treatment, there is currently no way to stop or even slow the progression of AD.<sup>1</sup> Drugs that are FDA approved, such as Namenda and Razadyne, only treat the symptoms associated with AD and become increasingly ineffective as the disease continues to progress.<sup>3</sup> Common effects of AD include disorientation, loss of long-term memory, deteriorating motor function and communication skills, and abrupt changes in behavior.<sup>1,4–6</sup>

The hallmarks of this disease, pathological neurofibrillary tangles and extracellular plaques, were first observed in 1907 by Alois Alzheimer.<sup>7</sup> The neurofibrillary tangles are composed of filamentous deposits of the tau protein while the extracellular plaques are fibrillary deposits of the amyloid- $\beta$  protein (A $\beta$ ). Since A $\beta$  is not found in other neurodegenerative disorders associated with tau such as Pick's disease, progressive supranuclear palsy, and corticobasal degeneration, tau dysfunction is not believed to lead to amyloid plaques.<sup>8,9</sup> When mice exhibiting both amyloid plaque and tau neurofibrillary

tangle pathology were immunized against A $\beta$ , levels of tau were also reduced.<sup>10</sup> Additionally, studies have demonstrated that A $\beta$  deposits appear first in AD mouse models,<sup>11</sup> further implicating that, although neurofibrillary tangles can induce severe neurodegeneration, it is the accumulation of A $\beta$  predominantly responsible for AD pathogenesis, making it a primary target for AD therapeutics.<sup>11-13</sup>

A $\beta$  is cleaved from the amyloid precursor protein (APP)<sup>14-17</sup> While its function is still unknown, A $\beta$  occurs naturally in blood, plasma, and cerebrospinal fluid and is not harmful in its monomeric form. In the case of AD, the monomeric form of A $\beta$  self-assembles into insoluble extracellular plaques characteristic of the disease. The two main isoforms of A $\beta$  contain 40 (A $\beta_{1-40}$ ) or 42 (A $\beta_{1-42}$ ) residues.<sup>18,19</sup> A $\beta_{1-40}$  is the more abundant isoform but is primarily found in vascular amyloid deposits, while A $\beta_{1-42}$ , the more hydrophobic of the two isoforms, deposits first in the brain and is more prone to aggregation and fibril formation.<sup>16,17</sup> While the A $\beta$  aggregation pathway has proved very complex and is still not completely understood, the basic A $\beta$  aggregation pathway is known to consist of lag, growth, and plateau phases (Figure 1.1). The aggregation begins when A $\beta$  undergoes nucleation, which is the rate limiting step of the aggregation process (lag phase).<sup>9,16</sup> Next, soluble A $\beta$  aggregates (which initiate as oligomers) continue to grow via lateral association and elongation by monomer addition until mature insoluble fibrils are formed, which deposit as plaques in the brain. Intervening in the aggregation pathway to either stop or slow the formation of aggregates has long been of interest as a therapeutic strategy.

## 1.2 The Damaging Effects of A $\beta$ Oligomers

Originally, large insoluble fibrils were believed to be the causative agent in AD progression; however, mounting evidence now supports that it is the smaller soluble oligomers that are primarily responsible. Neurological deficits associated with AD occur in the absence of fibrils in transgenic mouse models,<sup>20</sup> and the neurotoxic effect is independent of A $\beta$  plaque formation.<sup>21,22</sup> In contrast, the presence of A $\beta$  oligomers has been shown to cause neurodegeneration and correlates strongly with AD associated dementia.<sup>23-25</sup> Specifically, A $\beta$  oligomers can induce neurotoxicity,<sup>26</sup> synapse loss,<sup>27-29</sup> and impaired memory.<sup>30</sup> Our lab has previously demonstrated that small soluble A $\beta$  aggregates increase inflammatory responses, such as endothelial monolayer permeability, monocyte adhesion, and monocyte transmigration, while monomeric A $\beta$  and mature A $\beta$  fibrils are inert.<sup>31,32</sup>

Oxidative stress has also been implicated as a contributing factor to the cytotoxicity of A $\beta$ .<sup>33</sup> A $\beta$  has been shown to induce intracellular reactive oxygen species (ROS) which have proven capable of mediating cell signaling associated with A $\beta$ -induced cellular responses.<sup>34-36</sup> Furthermore, ROS is known to cause mitochondrial damage which can lead to caspase activation.<sup>37</sup> Caspases regulate vital cell networks responsible for inflammation and apoptosis.<sup>38</sup> Since A $\beta$  aggregates are foreign molecular structures, just their presence can trigger these inflammatory and apoptotic responses.<sup>39</sup> Studies have shown that A $\beta$  oligomers can activate NLRP3 inflammasome, a caspase promotor, and disrupt potassium channels leading to caspase-regulated inflammatory responses.<sup>39</sup> Additionally, AD patient's brain and plasma as well as transgenic AD mice show significant upregulation of caspase activation<sup>39</sup> Once activated, caspases have been shown to further the pathology of

AD by inducing tau cleavage, promoting tau tangle formulation, and cleaving APP.<sup>39</sup> Both ROS and caspase activation can be upregulated by A $\beta$  oligomers and have been studied for their role in AD, thus making the reduction of these cellular responses a key therapeutic strategy for AD.

### **1.3 Alteration of A $\beta$ Oligomers by Polyphenols as a Therapeutic Approach for AD**

Studies have demonstrated that both oligomer size and conformation effect oligomer induced cellular responses.<sup>40-42</sup> For example, lower molecular weight oligomers induce memory impairment associated with hippocampal synaptophysin while higher molecular weight oligomers induce greater oxidative stress.<sup>40</sup> Additionally, A $\beta$  oligomers of similar size but with different surface hydrophobicities<sup>41</sup> or conformations<sup>43</sup> elicit different toxic cellular responses. Therefore, compounds that are able to alter both A $\beta$  oligomer size distribution and conformation could reduce A $\beta$ -induced cellular toxicity.

Small molecules as inhibitors for A $\beta$  aggregation have been a focus since early studies showed that Congo red and thioflavin T, both small aromatic molecules, interact specifically with A $\beta$  fibrils and are capable of inhibiting fibril formation.<sup>44-46</sup> Polyphenols, compounds found in fruits, vegetables, and herbs, have attracted interest because of their aromatic structure and ability to serve as a natural therapeutic. Epidemiological studies have shown that diets rich in polyphenols result in a reduced incidence of AD.<sup>47-49</sup> Additionally, the aromatic carbon ring present in polyphenols has been shown to bind to A $\beta$  oligomers thereby preventing further aggregation.<sup>50,51</sup> Many polyphenols have demonstrated the ability to obstruct the A $\beta$  aggregation pathway, including quercetin,<sup>52</sup> resveratrol,<sup>53</sup> myricetin,<sup>52</sup> curcumin,<sup>54</sup> and piceid.<sup>55</sup> Polyphenols also bind to many proteins altering the protein aggregate conformation.<sup>56</sup> MegaNatural-AZ, a polyphenol derived

from grape seed, and oleocanthal, a phenolic compound found in olive oil, both effect A $\beta$ -induced cellular toxicity by altering A $\beta$  aggregate conformation.<sup>57,58</sup> Combined, these studies suggest that polyphenols have the potential to reduce A $\beta$ -induced cellular responses by altering A $\beta$  oligomer formation.

#### **1.4 Polyphenols' Antioxidant Capabilities as a Therapeutic Approach for AD**

Antioxidants have been studied as treatments for oxidative-stress-induced cellular apoptosis observed in several neurodegenerative diseases including AD, Parkinson's disease, and stroke.<sup>33</sup> It has further been demonstrated that antioxidants, which neutralize ROS, have the ability to inhibit A $\beta$  cytotoxicity.<sup>59,60</sup> Polyphenols serve as the most abundant antioxidants in diet<sup>61</sup> and their antioxidant capabilities are believed to play a role in their ability to effect various diseases.<sup>62-64</sup> Many polyphenols have demonstrated the ability to neutralize the increased ROS induced by A $\beta$  aggregates.<sup>44,47,65-67</sup> This observation suggests that polyphenols could act as effective inhibitors of A $\beta$ -induced cellular responses by attenuating increased ROS, giving polyphenols the potential to act as dual action therapeutics for AD by both altering A $\beta$  oligomer formation and reducing ROS.

#### **1.5 Study Overview**

This study investigated the hypothesis that polyphenols can act as dual action therapeutics for AD by acting through two separate mechanisms: 1) by altering A $\beta$  oligomer formation and 2) by reducing ROS through antioxidant capabilities. Before dual action capabilities could be assessed, polyphenols' ability to act through each mechanism was investigated separately. These studies as well as the dual action study make up the three primary aims of this work and are described below.

### *1.5.1 Polyphenols attenuate A $\beta$ -induced cellular responses by altering oligomer size and conformation*

This aim tests the hypothesis that polyphenols present during A $\beta$  oligomer formation will alter the resulting oligomers by either changing the oligomer size distribution and/or altering oligomer conformation. Furthermore, this aim determines if these oligomer alterations attenuate A $\beta$ -induced cellular responses. The size distribution of oligomers formed in the absence or presence of polyphenols was analyzed using SDS-PAGE and Western blot while the resulting oligomer conformation was examined using either ANS or Nile Red spectroscopy. The effect these changes have on A $\beta$ -induced cellular responses was evaluated by comparing intracellular ROS and caspase activity in neuroblastoma cells treated with A $\beta$  oligomers formed in the absence or presence of selected polyphenols.

### *1.5.2 Polyphenols attenuate A $\beta$ -induced cellular responses by reducing intracellular ROS through their antioxidant capabilities*

This aim tests the hypothesis that polyphenols' antioxidant capabilities can attenuate A $\beta$ -induced intracellular ROS and that this reduction in ROS also decreases caspase activation. Polyphenols with high antioxidant capability were identified through an oxygen radical absorbance capacity (ORAC) assay. As in Aim 1, an intracellular ROS assay was employed, this time to ensure that the high antioxidant capabilities translated into a reduction of intracellular ROS induced by A $\beta$  oligomers. Additionally, the effect that the reduction of ROS had on A $\beta$  oligomer induced caspase activation was investigated by comparing the caspase activity in cells treated with A $\beta$  oligomers alone to cells treated

simultaneously with A $\beta$  oligomers and polyphenols at a concentration shown to reduce intracellular ROS.

### *1.5.3 Polyphenols can act as dual action therapeutics for AD by both altering A $\beta$ oligomer formation and by reducing intracellular ROS.*

This aim tests the hypothesis that polyphenols that exhibit both mechanisms of inhibition, alteration to A $\beta$  oligomer formation and neutralization of intracellular ROS, can act as dual action inhibitors against A $\beta$ -induced cellular responses. To explore the potential of dual action between the two mechanisms, cells were treated with oligomers formed in the presence of polyphenols along with enough additional polyphenol to allow for ROS inhibition. Polyphenols that reduced intracellular ROS and/or caspase activation by a greater amount than the reduction seen in the first and second aims were identified as dual action therapeutics for AD.

These three hypotheses were tested using two separate sets of polyphenols. The first set, discussed in Chapter 3, was selected in order to evaluate the effect that hydroxyl placement on the polyphenol ring structure has on inhibitory capability. The second set, discussed in Chapter 4, investigates the changes in inhibitory capability when a polyphenol is metabolized resulting in the replacement of a hydroxyl group with a methoxy group on the polyphenol ring.

## **1.6 Innovation**

While epidemiological studies support the ability of polyphenols to attenuate AD,<sup>47-49</sup> further studies are needed to elucidate the mechanism by which polyphenols intervene in the disease process. This research investigates two mechanisms by which polyphenols can inhibit the cellular responses caused by A $\beta$ . The first mechanism, altering

oligomer formation, has not been fully explored, with most studies focusing on polyphenols' ability to inhibit the formation of fibrils, the last stage of the aggregation process.<sup>52,53,55,68–70</sup> More data is needed on the ability of polyphenols to inhibit the early stages of aggregation, specifically oligomer formation, which is thought to be the A $\beta$  species primarily responsible for pathogenesis.<sup>23,24</sup> This study also aids in determining if inhibition of fibril formation coincides with inhibition of oligomerization or if these inhibitory effects are achieved by independent mechanisms. Additionally, this study gains insight into which polyphenol subclass and functionalization is most effective at modulating oligomerization by exploring an array of polyphenol structures.

Reduction of A $\beta$ -induced intracellular ROS through antioxidant capabilities is the second mechanism that is explored. Various studies have evaluated the antioxidant capabilities of extracts from foods rich in polyphenols;<sup>71–73</sup> however, this study determines the antioxidant capabilities of isolated polyphenols and the effect these capabilities have on A $\beta$ -induced intracellular ROS. This study also investigated the importance of A $\beta$ -mediated ROS second messengers to caspase activity and the ability of polyphenols to counteract this process.

While polyphenols have been studied previously for both of the described inhibitory mechanisms, which mechanism is most effective at reducing A $\beta$ -induced cellular responses is unknown. This study gains insight into the predominant inhibitory mechanism as well as determines the ability of these two mechanisms to work together to reduce A $\beta$  induced cellular responses. The combined results of this study will direct future work in identifying the best natural therapeutics for AD and will identify effective polyphenols to use as lead compounds for therapeutic development.

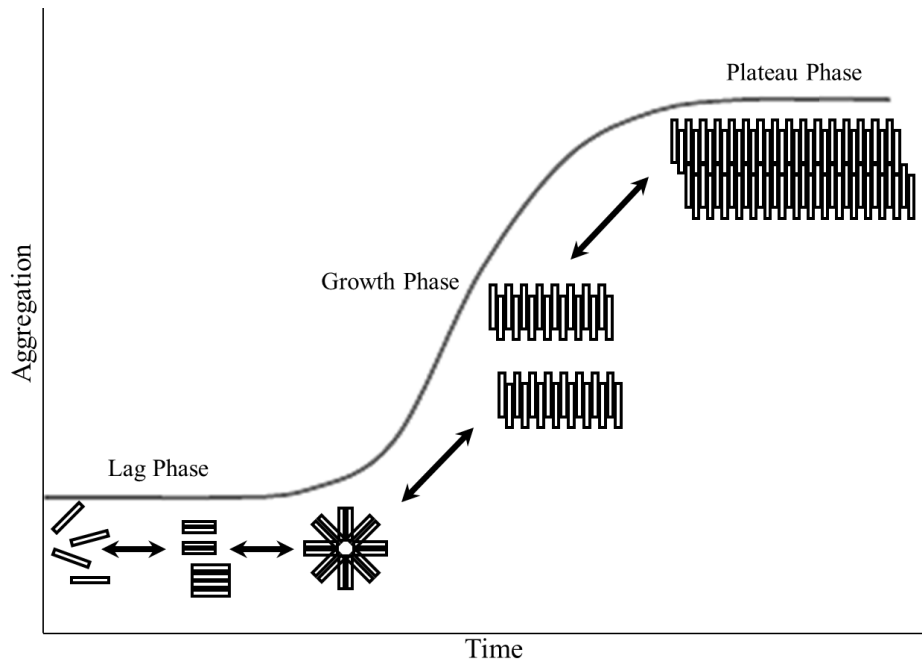


**Figure 1.1 The progression of A $\beta$  aggregation.** A $\beta$  monomer undergoes a rate-limiting nucleation lag phase followed by growth of soluble aggregates. These aggregates can then elongate or associate to form insoluble fibrils. Finally a plateau is reached where fibrils, soluble aggregates, and monomers are in equilibrium. Double arrows indicate equilibrium reactions.

## CHAPTER 2

### MATERIALS AND METHODS

#### **2.1 Materials**

$\text{A}\beta_{1-42}$  was purchased from AnaSpec, Inc. (San Jose, CA), and the OxiSelect<sup>TM</sup> Oxygen Radical Antioxidant Capacity (ORAC) activity assay was purchased from Cell Biolabs (San Diego, CA). Lamilli buffer, Tricene sample buffer, 4-20% tris-glycine gels, 16.5% tris-tricine gels, Precision Plus Protein WesternC standard, Precision Plus Protein Dual Xtra standard, and 0.2  $\mu\text{m}$  nitrocellulose membrane were purchased from Bio-Rad (Hercules, CA). Monoclonal antibody 6E10 was obtained from Covance (Princeton, NJ). 1, 1, 1, 3, 3, 3-hexafluoro-2-propanol (HFIP) was purchased from Sigma Aldrich (St. Louis, MO). 8-anilino-1-naphthalenesulphonic acid (ANS) was obtained from Research Organics (Cleveland, OH). HRP-conjugated anti-mouse secondary antibody, dimethyl sulfoxide (DMSO), Tween-20 and chemiluminescent reagents were purchased from VWR (Radnor, PA). Nile Red, the Image-iT LIVE Green poly-caspase kit, and 2', 7' dichlorodihydrofluoescin diacetate (DCFH-DA) were purchased from Life Technologies (Carlsbad, CA).

#### **2.2 Preparation of $\text{A}\beta_{1-42}$ Oligomers**

$\text{A}\beta_{1-42}$  was reconstituted in cold HFIP to 4 mg/mL and incubated on ice for 60 min. The protein solution was aliquoted, and the HFIP was allowed to evaporate overnight at 25 °C. Resulting protein films were stored at -80 °C until use. To form  $\text{A}\beta_{1-42}$  oligomers, protein films were reconstituted in DMSO to 1.5 mM and combined with 10-fold molar

excess polyphenol (prepared fresh at 10mM in DMSO) or an equivalent volume of DMSO (control). To initiate oligomerization, 12 mM phosphate buffer (pH 7.4) containing 1  $\mu$ M NaCl was added to the sample for a final concentration of 15  $\mu$ M A $\beta$ <sub>1-42</sub>, 150  $\mu$ M polyphenol, and  $\leq$  2.5% DMSO. Following 30 min incubation (25 °C), reactions were stabilized by the addition of Tween-20 (final concentration of 0.1%) for SDS-PAGE and Western blot analysis or were immediately diluted for ANS spectroscopy, Nile Red spectroscopy, or cell culture assays.

### **2.3 Determination of A $\beta$ <sub>1-42</sub> Oligomer Size via SDS-PAGE and Western Blot**

To determine whether polyphenols present during oligomerization alter oligomer size distribution, Tween-20 stabilized oligomers formed in the absence (control) or presence of polyphenols were mixed 1:1 with Lamilli buffer for size characterization using SDS-PAGE and Western blot. For quantification of oligomers 25-250 kDa in size, samples were loaded onto a 4-20% Tris-glycine gel and electrophoresed (120 V) using a Mini-PROTEAN Tetra Cell (Bio-rad). Precision Plus Protein WesternC standard was used for size determination. Protein was electrotransferred (14 V, 12 min) onto 0.2  $\mu$ m nitrocellulose membrane (Bio-Rad) using a Trans-blot SD semi-dry transfer cell (Bio-Rad). For quantification of monomer, trimer, and tetramer bands, stabilized oligomers were instead mixed 1:2 with Tricene sample buffer, loaded onto a 16.5% Tris-tricine gel, electrophoresed (100V), and electrotransferred (13 V, 12 min) onto 0.2  $\mu$ m nitrocellulose membrane. Precision Plus Protein Dual Xtra standard was used for band determination.

Membranes were blocked (overnight, 4 °C) in 5% dry nonfat milk in 0.002% Tween phosphate buffered saline (PBS-T) and probed (1 h) with 6E10 monoclonal antibody

(1:2000), a sequence-specific antibody which binds to the N-terminal region of A $\beta$  not involved in aggregation. After washing the membrane 3 times for 5 min with PBS-T, HRP-conjugated anti-mouse secondary antibody (1:2000) and Precision Protein StrepTactin-HRP conjugate (1:2000) were allowed to bind for 45 min. The membrane was again washed with PBS-T and placed in enhanced chemiluminescent reagents for 2 min. Images were obtained using the Gel DocTM XRS+ imaging system (Bio-Rad). Image Lab software (Bio-Rad) was used to quantify the volume intensity for larger (250 kDa-100 kDa) and smaller oligomers (100 kDa-25 kDa) and to quantify the band intensity for monomer, trimer, and tetramer bands. Intensity values for each range are reported as a fraction of the control.

#### **2.4 Assessment of A $\beta$ <sub>1-42</sub> Oligomer Conformation via ANS Spectroscopy**

ANS spectroscopy was used to determine if the presence of polyphenols during oligomerization altered the resulting oligomer conformation. ANS, which binds to exposed hydrophobic molecular surfaces resulting in both a blue shift and increase in fluorescence, has been used extensively in protein folding to identify the presence of exposed hydrophobic patches and has been used to evaluate the extent of exposed hydrophobic residues on the surface of A $\beta$  aggregates, including oligomers, as an indication of aggregate conformation.<sup>74-76</sup> ANS was solubilized in DMSO at 50 mM and stored at 4 °C. ANS was further diluted in 12 mM phosphate buffer (pH 7.4) and added to oligomers made in the absence (control) or presence of polyphenols for final concentrations of 1  $\mu$ M A $\beta$ <sub>1-42</sub>, 10  $\mu$ M polyphenol, and 100  $\mu$ M ANS. Fluorescence emission from 400 nm-600 nm with excitation at 350 nm was measured using an LS-45 luminescence spectrophotometer (Perkin Elmer, Waltham, MA). Fluorescence values were determined as the integrated

area under the curve (IAUC) from 450-550 nm with blank (buffer or polyphenol with ANS) subtraction. Results are normalized to the control.

## **2.5 Assessment of A $\beta$ <sub>1-42</sub> Oligomer Conformation via Nile Red Spectroscopy**

For polyphenols exhibiting a self-fluorescence in the ANS wavelength range, Nile Red was used as an alternative probe to determine if polyphenols present during oligomerization alter the resulting oligomer conformation. Nile Red is a dye which, similar to ANS, emits an increased fluorescent intensity with a blue shift when in the presence of exposed non-polar molecular surfaces. Nile Red has also been used previously for the analysis of A $\beta$  aggregate surface hydrophobicity as an indicator of conformation change.<sup>77,78</sup> A 2.5 mM stock of Nile Red was prepared by dissolving Nile Red in ethanol. Nile Red was further diluted in phosphate buffer (pH 7.4) to 150  $\mu$ M and combined with oligomers made in the absence (control) or presence of polyphenols for final concentrations of 5  $\mu$ M A $\beta$ <sub>1-42</sub>, 50  $\mu$ M polyphenol, and 100  $\mu$ M Nile Red. Fluorescence was measured and results analyzed in the same fashion as described for ANS (Section 2.4) but using an excitation of 550 nm and emission from 580-700 nm with the IAUC being calculated from 580-700 nm.

## **2.6 Determination of Polyphenols' Antioxidant Capacity via ORAC Assay**

Antioxidant capacities of polyphenols were assessed using the ORAC assay. Briefly, freshly dissolved polyphenol stock solutions (10 mM in DMSO) and Trolox, a vitamin E analog and strong antioxidant, standards were diluted in 75 mM potassium phosphate (pH 7.0) such that all samples and standards contained <5% DMSO (v/v). Samples and standards were mixed in a 1:6 ratio with fluorescein probe and incubated at 37 °C for 30 min. Free radical initiator was then added at a concentration of 80 mg/mL,

and fluorescence readings were obtained using a Synergy 2 multi-detection microplate reader (BioTek, Winooski, VT). Fluorescence at  $480 \pm 20$  nm excitation and  $520 \pm 20$  nm emission was measured under temperature controlled conditions ( $37^\circ\text{C}$ ) at 1 min intervals until the fluorescence returned to baseline (1 h). Fluorescence was plotted versus time and the integrated area under the curve (IAUC) with blank (buffer) subtraction was determined. This net IAUC was converted to an equivalent Trolox concentration using the Trolox standard curve. Results are reported as the ORAC value, which is the equivalent Trolox concentration per unit concentration of polyphenol.

## **2.7 Media and Cell Lines**

Human neuroblastoma SH-SY5Y cells (American Type Culture Collection, Manassas, VA) were maintained in a 1:1 mixture of Ham's F12K medium and DMEM. Medium was supplemented with 10% FBS, 100 units/mL penicillin, and 100  $\mu\text{g}/\text{mL}$  streptomycin. All cultures were maintained at  $37^\circ\text{C}$  in a humid atmosphere of 5%  $\text{CO}_2$  and 95% air.

## **2.8 Analysis of Polyphenols' Ability to Reduce Oligomer-Induced Intracellular ROS via DCFH-DA Assay**

A DCFH-DA fluorescent probe was implemented to determine the effectiveness of polyphenols at decreasing  $\text{A}\beta$ -induced intracellular ROS. SH-SY5Y cells were seeded at a density of  $5 \times 10^4$  cells/well onto black-sided 96-well tissue culture plates (VWR) and were maintained for 24 h in F12K/DMEM, supplemented as described in Section 2.7. Cells were subsequently exposed to varying treatments of  $\text{A}\beta_{1-42}$  oligomers and polyphenol diluted in 1% FBS, phenol-red free (PRF) media. Cells treated with buffer equivalent (phosphate buffer, <0.5% DMSO) or 25  $\mu\text{M}$   $\text{H}_2\text{O}_2$  served as a vehicle and positive control,

respectively. Cells treated with polyphenol alone ensured there was no change to basal ROS levels (data not shown). After 24 h incubation (37 °C, 5% CO<sub>2</sub>), treatments were removed, and cells were incubated for 30 min (37 °C, 5% CO<sub>2</sub>) with DCFH-DA diluted in PRF, serum free media. Cellular uptake and deacetylation of DCFH-DA and subsequent oxidation by intracellular ROS leads to a conversion to highly fluorescent 2', 7' dichlorodihydrofluorescein (DCF). The resulting fluorescence was measured (Synergy 2 multi-detection microplate reader) at excitation and emission wavelengths of 480±20 nm and 530±25 nm, respectively. Fluorescent values were converted to DCF concentration using a DCF standard curve.

### **2.9 Analysis of Polyphenols' Ability to Reduce Oligomer-Induced Caspase Activation**

The Image-iT LIVE Green Poly Caspases detection kit (Life Technologies, Carlsbad, CA), which implores a fluorescent inhibitor of caspases (FLICA) reagent for detection of caspase-1, -3, -4, -5, -6, -7, -8 and -9 as well as Hoechst 33342 for labeling of nuclei, was used to determine the ability of Aβ<sub>1-42</sub> oligomers to induce caspase activation as well as the ability of polyphenols to attenuate this response. SH-SY5Y cells were seeded at a density of 1 x 10<sup>6</sup> cells/well onto 22 x 22 mm glass coverslips in 6-well tissue culture plates and were maintained for 24 h in F12K/DMEM, supplemented described in Section 2.7. Cells were subsequently exposed to varying treatments of Aβ<sub>1-42</sub> oligomers and polyphenol diluted in 1% FBS media. Cells treated with polyphenol alone ensured there was no change to basal caspase levels (data not shown). Cells treated with buffer equivalent or 1.5 U/μL TNF-α served as vehicle and positive controls, respectively.

Following 24 h incubation (37 °C, 5% CO<sub>2</sub>), treatment was removed, and cells were rinsed with PRF media containing 1% FBS then incubated (37 °C, 5% CO<sub>2</sub>) for 1 h

with FLICA stain (diluted from 150X to 30X using PBS then to 1X using PRF media containing 1% FBS). Following incubation, the stain was removed, and cells were washed twice with media before 10 min incubation (37 °C, 5% CO<sub>2</sub>) with Hoechst 33342 stain (diluted 1:1000 in PRF media containing 1% FBS). The cells were then washed twice with wash buffer and mounted to slides using the kit's fixative solution. Labeled cells were imaged approximately 2 h after staining under a Nikon Eclipse 80i fluorescent microscope using a 40x objective. For each slide, 5 different fields were captured for analysis. For each field, both a Hoechst image and FLICA image were acquired.

Using the Hoechst images, a custom subroutine written in Matlab (Mathworks, Natick, MA) was used to quantify the total number of cells and determine the individual caspase activity of each cell. The subroutine used Hoechst images to tag pixels representative of the boundaries of nuclei and then iteratively identified successive 'layers' of pixels moving further into the interior of the cell. Once iterations were completed and convergence detected, each cell was counted. A radius of exclusivity was defined for each cell within which another cell could not be identified. Parameters used by the algorithm were calibrated to statistically produce the same values as manual cell counts. The subroutine then utilized the nuclei boundaries (determined from the Hoechst images) to evaluate within FLICA images the average caspase pixel intensity within each nucleus plus a specified region outside the nucleus, to account for caspase staining in the cytoplasm. Cells displaying an average caspase pixel intensity above 5 were deemed as caspase active. The full Matlab code and an example output from the code can be found in Appendixes A and B, respectively. For each treatment approximately 300 – 600 cells were analyzed. Caspase activation is reported as the fraction of caspase activated cells which is defined as

the total number of caspase active cells (FLICA) divided by the total number of cells (Hoechst).

## **2.10 Statistical Analysis**

Prism 5 software (Graphpad Software, La Jolla, CA) was used for all statistical analysis. A one-way analysis of variance (ANOVA) was used to compare all samples to the respective control, and an unpaired t-test was used for comparison between samples.  $p<0.05$  was considered significant. All values are expressed as the mean  $\pm$  SEM.

## CHAPTER 3

### POLYPHENOLS ATTENUATE A $\beta$ OLIGOMER-INDUCED CELLULAR RESPONSES

#### 3.1 Introduction

Polyphenols have attracted attention as possible natural therapeutics for AD based on epidemiological studies showing correlations between polyphenol-rich diets and reduced incidence of AD (Section 1.3).<sup>47-49</sup> Polyphenols contain a two aromatic carbon ring structure the presence of which in other compounds has shown the ability to bind to A $\beta$  oligomers thereby preventing further aggregation.<sup>50,79</sup> While studies have demonstrated that various polyphenols have the ability to obstruct the A $\beta$  aggregation pathway,<sup>53,55,80</sup> these studies have been primarily focused on inhibiting the formation of fibrils not the more damaging oligomers.

Another potential advantage of using polyphenols for AD treatment is their antioxidant properties (discussed further in Section 1.4). ROS has been implicated as a contributing factor in neurodegenerative diseases and the cytotoxicity of A $\beta$ ,<sup>33,81,82</sup> making the reduction of ROS one therapeutic approach for AD. Some polyphenols have demonstrated the ability to neutralize the increased ROS induced by A $\beta$  aggregates.<sup>83</sup> Together, the observed anti-aggregation and antioxidant capabilities of polyphenols suggest that these natural compounds could potentially act as dual-action therapeutics for AD.

This chapter investigates the polyphenols flavone (FLA), apigenin (API), luteolin (LUT), kaempferol (KAE), and quercetin (QUE) (Figure 3.1), which are found in an

assortment of foods such as herbs, apples, berries, celery and peppers. These compounds have been examined for their potential health benefits in a number of areas including anti-ulcer<sup>84–86</sup> anti-inflammatory<sup>84,87</sup>, anti-spasmodic<sup>85,86</sup> and anti-cancer.<sup>84,88,89</sup> This study investigates the ability of these polyphenols to attenuate the toxic effect of A $\beta$  oligomers by two mechanisms 1) altering oligomer formation by changing oligomer size distribution and/or modulating oligomer conformation and 2) reducing A $\beta$  oligomer-induced ROS through antioxidant capabilities. The ability of polyphenols to act as dual-action therapeutics by acting through both mechanisms was also explored.

The ability of polyphenols to alter oligomer size distribution was found to be heavily dependent on hydroxyl placement on the polyphenol, with a hydroxyl group on the 3 position being crucial for oligomer inhibition. Polyphenols were also found to be able to modulate oligomer conformation in varying ways with LUT decreasing oligomer surface hydrophobicity and QUE increasing oligomer surface hydrophobicity. Altering oligomer conformation, rather than altering oligomer size distribution, appears to play a key role in reducing oligomer-induced intracellular ROS, with LUT being the only polyphenol capable of reducing intracellular ROS by altering oligomer formation. All of the polyphenols however were able to significantly reduce oligomer-induced ROS through their antioxidant properties. The antioxidant capability of LUT and QUE also resulted in a reduction of oligomer-induced caspase activity. These results indicate that A $\beta$ -mediated ROS second messengers play a role in caspase activation and that strong antioxidants can counter-act these effects. KAE was one of the most noteworthy polyphenols, exhibiting dual-action reduction of both ROS and caspase activity. Together these findings demonstrate the relationship between oligomer-induced ROS and caspase activity, identify

promising polyphenols as natural therapeutics for AD, indicate the dominant mechanism by which polyphenols attenuate A $\beta$ -induced cellular responses, and identify KAE as a potential dual-action therapeutic for AD.

### **3.2 Materials and Methods**

#### *3.2.1 Preparation of Polyphenols*

Polyphenols FLA, KAE, and QUE were purchased from Sigma Aldrich (St. Louis, MO), while API and LUT were purchased from Indofine Chemical Company (Hillsborough Township, NJ). All polyphenols were freshly dissolved in DMSO to a concentration of 10 mM to be used in experiments.

#### *3.2.2 Preparation of A $\beta$ <sub>1-42</sub> Oligomers*

A $\beta$ <sub>1-42</sub> oligomers were formed in the absence (control) or 10-fold excess of either FLA, API, LUT, KAE or QUE, as described in Section 2.2.

#### *3.2.3 Determination of A $\beta$ <sub>1-42</sub> Oligomer Size via SDS-PAGE and Western blot*

To determine whether polyphenols present during oligomerization alter oligomer size distribution, SDS-PAGE with Western blotting was performed as described in Section 2.3. Image Lab software was used for quantification of both larger (250 kDa – 100 kDa) and smaller (100 kDa – 25 kDa) oligomers as well as monomer, trimer, and tetramer species. Intensity values for each range are reported as a fraction of the control (oligomers formed in absence of polyphenol).

#### *3.2.4 Assessment of A $\beta$ <sub>1-42</sub> Oligomer Conformation via ANS Spectroscopy*

ANS spectroscopy was used as described in Section 2.4 to determine if the presence of polyphenols during oligomerization altered the resulting oligomer conformation. Fluorescence values were determined as the IAUC from 450-550 nm with blank (buffer or

polyphenol with ANS) subtraction. The effect KAE has on oligomer conformation was unable to be tested via ANS due to the self-fluorescence associated with this polyphenol. Results are normalized to control oligomers.

### *3.2.5 Assessment of Polyphenol Antioxidant Capacity via ORAC Assay*

Antioxidant capacities of polyphenols were assessed using the ORAC assay as described in Section 2.6. Results are reported as the ORAC value, which is the equivalent Trolox concentration per unit concentration of polyphenol.

### *3.2.6 Evaluation of A $\beta$ <sub>1-42</sub> Oligomer-Induced Intracellular ROS*

An OxiSelect™ intracellular ROS assay kit was implemented to assess the ability of oligomers to increase intracellular ROS as well as the effectiveness of polyphenols to attenuate this increase. SH-SY5Y cells were seeded and maintained as described in Sections 2.7 and 2.8. To determine the effect that polyphenol-induced changes in oligomer size and conformation had on A $\beta$ -induced intracellular ROS, A $\beta$ <sub>1-42</sub> oligomers formed in the presence or absence (control) of polyphenols were diluted in 1% FBS, PRF media and added to cells at final concentrations of 0.01  $\mu$ M A $\beta$ <sub>1-42</sub> oligomers and 0.1  $\mu$ M polyphenol. To assess the effectiveness of polyphenols' antioxidant capabilities at decreasing A $\beta$ -induced intracellular ROS, cells were treated simultaneously with 40  $\mu$ M polyphenol and 0.01  $\mu$ M control A $\beta$ <sub>1-42</sub> oligomers. Additionally, cells were treated with 0.01  $\mu$ M A $\beta$ <sub>1-42</sub> oligomers formed in the presence of polyphenol plus an additional 40  $\mu$ M polyphenol to determine the potential of polyphenols to serve as dual-action therapeutics by reducing A $\beta$ -induced intracellular ROS via both mechanisms (altering oligomer formation and antioxidant capability). Intracellular ROS was assessed as described in Section 2.8.

Resulting fluorescent values were blank subtracted and converted to DCF concentration using a DCF standard curve.

### *3.2.7 Evaluation of A $\beta$ <sub>1-42</sub> Oligomer-Induced Caspase Activation*

The Image-iT LIVE Green Poly Caspases detection kit was used as described in Section 2.9 to determine the ability of polyphenols to attenuate A $\beta$ <sub>1-42</sub> oligomer-induced caspase activation. SH-SY5Y cells were seeded and maintained as described in Sections 2.7 and 2.9 and then exposed to varying treatments of 0.01  $\mu$ M A $\beta$ <sub>1-42</sub> oligomers and 40  $\mu$ M polyphenol diluted in 1% FBS media as described in Section 3.2.6 for the intracellular ROS assay. Caspase activation is reported as the fraction of caspase activated cells which is defined as the total number of caspase active cells (FLICA) divided by the total number of cells (Hoechst).

## **3.3 Results**

### *3.3.1 Polyphenols alter A $\beta$ oligomer size distribution*

To evaluate the ability of polyphenols to alter oligomerization, A $\beta$ <sub>1-42</sub> oligomers were formed in the absence (control) or presence of each polyphenol. The size distribution of the resulting oligomers was assessed using SDS-PAGE and Western blot. When separation was performed on a 4-20% Tris-glycine gel (Figure 3.2 A), only FLA was unable to reduce the formation of oligomers in both the 250-100 kDa (Figure 3.2 B) and 100-25 kDa (Figure 3.2 C) size ranges, indicating that the presence of hydroxyl groups is crucial for disruption of oligomerization. API, LUT, KAE, and QUE all significantly reduced the quantity of 250-100 kDa oligomers (Figure 3.2 B), with KAE exhibiting the most pronounced effect, a >95% reduction. Additionally, both flavonols (KAE and QUE) were significantly more effective at reducing the formation of 250-100 kDa oligomers than

the flavones (API and LUT), demonstrating that the hydroxyl at the 3 position is important to the inhibition process. Conversely, when comparing API and KAE to their 3' hydroxylated analogs (LUT and QUE, respectively), no significant difference in 250-100 kDa oligomers is observed, suggesting that the hydroxyl at this position is less crucial for inhibition.

API, KAE, and QUE also significantly reduced the formation of 100-25 kDa oligomers (Figure 3.2 C). Again, KAE exhibited the most pronounced inhibition, reducing formation of these oligomers by nearly 65%. Interestingly, addition of a hydroxyl at the 3' position, to convert API to LUT, results in a loss of inhibitory effect; however, addition of a hydroxyl at the 3 position, to convert LUT to QUE, regains this inhibitory capability. Furthermore, moving the hydroxyl from the 3' position to the 3 position, to convert LUT to KAE, also regains this inhibitory capability. Together, these results demonstrate the importance of hydroxyl placement to the inhibitory capabilities of polyphenols and support the importance of a hydroxyl at the 3 position.

When separation was performed on a 16.5% Tris-tricine gel (Figure 3.2 D), none of the polyphenols examined significantly altered the amount of tetramer formed (Figure 3.2 E), and only the presence of FLA and KAE resulted in a significant decrease in trimer formation (Figure 3.2 F). Dimer species were not evaluated as they have been shown to be effected by SDS when crosslinking is not employed to stabilize the dimer structure.<sup>90</sup> The most pronounced polyphenol-induced change occurred in the amount of monomeric A $\beta$  present (Figure 3.2 G), with all polyphenol samples except QUE exhibiting significantly less monomer than the control. Together, the decrease in monomer, trimer, and tetramer species observed when oligomers are formed in the presence of API, LUT,

and KAE could indicate that the concomitant reduction of 250-25 kDa oligomers is caused by shifting the oligomer size distribution into higher molecular weight aggregates. Additionally, polyphenols may not directly bind to small A $\beta$  species but instead interact primarily with A $\beta$  oligomers.

### *3.3.2 Polyphenols modulate A $\beta$ oligomer conformation*

To determine whether the presence of polyphenols during oligomerization alters oligomer conformation, A $\beta$ <sub>1-42</sub> oligomers formed in the absence (control) or presence of each of the polyphenols were assessed for alterations in surface hydrophobicity using ANS. This fluorescent dye binds to exposed hydrophobic residues to give a shifted and enhanced fluorescence (Figure 3.3 A-D). Oligomers formed in the presence of LUT exhibited significantly less surface hydrophobicity than oligomers formed alone, while oligomers formed in the presence of QUE exhibited significantly higher surface hydrophobicity when compared to the control (Figure 3.3 F). Thus, polyphenols not only modulate oligomer conformation but do so in varying ways. Oligomers were unchanged in conformation by FLA and API, again demonstrating the importance of polyphenol hydroxyl placement to polyphenol modulation of oligomerization.

### *3.3.3 A $\beta$ oligomers increase intracellular ROS and caspase activity in human neuroblastoma cells*

To verify the physiological activity of A $\beta$ <sub>1-42</sub> oligomers, their ability to increase intracellular ROS and stimulate caspase activity was evaluated using SH-SY5Y neuroblastomas cells. Levels of intracellular ROS were assessed using the DCFH-DA probe, which undergoes intracellular metabolism by ROS to fluorescent DCF. When cells were treated for 24 h with 0.01  $\mu$ M A $\beta$ <sub>1-42</sub> oligomers, a 50% increase in intracellular

ROS was observed over cells exposed to buffer equivalent (vehicle) (Figure 3.4 A). In fact, this increase in intracellular ROS is similar to that observed for cells treated with 25  $\mu$ M H<sub>2</sub>O<sub>2</sub>, a known inducer of intracellular ROS.<sup>91-93</sup> Similarly, 24 h exposure of SH-SY5Y neuroblastoma cells to 0.01  $\mu$ M A $\beta$ <sub>1-42</sub> oligomers stimulated caspase activity. While cells treated with buffer equivalent (vehicle) displayed negligible caspase activation, approximately 50% of the cells treated with A $\beta$  oligomers exhibited caspase activity (Figures 3.4 B-C). The level of A $\beta$ <sub>1-42</sub> oligomer-induced caspase activation paralleled that observed for cells exposed to 1.5 U/ $\mu$ L TNF- $\alpha$ , shown previously to induce caspase in neuronal cell models.<sup>94-96</sup> Together, these results demonstrate the damaging physiological effects of oligomers at nanomolar A $\beta$  concentrations.

### *3.3.4 Polyphenols exhibit antioxidant capacity*

The antioxidant capability of polyphenols was evaluated using an ORAC assay, which employs a fluorescent probe that is subject to decay in the presence of free radicals. As a result, prolonged fluorescence upon incubation with a polyphenol is indicative of antioxidant capacity. All polyphenols presented strong antioxidant capacity (Figure 3.5 A), with FLA, API, LUT, and KAE exhibiting a capacity similar to that of the Trolox standard and QUE exhibiting a significantly higher antioxidant capacity than Trolox. In addition, both API and QUE displayed significantly greater antioxidant capacity than LUT and KAE, demonstrating the influence of hydroxyl placement upon polyphenol antioxidant capacity.

### *3.3.5 Polyphenols reduce A $\beta$ oligomer-induced intracellular ROS*

As evidenced by the data above, polyphenols modulate oligomer formation and possess strong antioxidant capability and therefore may have the potential to attenuate A $\beta$

oligomer-induced intracellular ROS (Figure 3.4 A). In addition, these mechanisms may work in concert to synergistically reduce this increase in ROS. Each of these possibilities was examined using the DCFH-DA probe to assess intracellular ROS following cellular treatments designed to isolate these individual mechanisms of action.

To determine if the observed alterations to oligomer size (Figure 3.2) and conformation (Figure 3.3) can attenuate oligomer-induced intracellular ROS, A $\beta$ <sub>1-42</sub> oligomers were prepared in the presence of 10-fold excess polyphenol and diluted to 0.01  $\mu$ M for cellular treatment. When intracellular ROS was evaluated following 24 h treatment, only LUT was able to significantly reduce A $\beta$  oligomer-induced intracellular ROS (Figure 3.5 B, open bars). Additionally, simultaneous treatment (24 h) of cells with 40  $\mu$ M polyphenol and 0.01  $\mu$ M A $\beta$ <sub>1-42</sub> oligomers formed in the absence of polyphenol was performed to probe whether the observed polyphenol antioxidant capacity (Figure 3.5 A) can attenuate oligomer-induced intracellular ROS. Here, all compounds significantly lowered A $\beta$  oligomer-induced intercellular ROS (Figure 3.5 B, closed bars). Treatments including API, LUT, or QUE exhibited ~50% reduction in ROS, while KAE proved inferior to these compounds ( $p<0.05$ ), eliciting the weakest ability to reduce intracellular ROS through antioxidant capabilities. FLA was also inferior to API and LUT at reducing A $\beta$  oligomer-induced intracellular ROS through antioxidant capabilities ( $p<0.05$  and  $p<0.01$ , respectively).

To determine whether polyphenols can act through these two mechanisms in concert to decrease A $\beta$  oligomer-induced intracellular ROS, cells were treated simultaneously with 40  $\mu$ M polyphenol and 0.01  $\mu$ M A $\beta$ <sub>1-42</sub> oligomers formed in the presence of polyphenol. All treatments conferred a significant reduction in intracellular

ROS relative to cells treated with oligomers alone (Figure 3.5 B, grey bars). Among treatments, FLA was again inferior to its hydroxylated counterparts. Moreover, when these dual-mechanism treatments included FLA, API, LUT, or QUE, the exhibited ROS reduction was similar to that observed for cellular treatment designed to isolate antioxidant capability. Combined, these results demonstrate that polyphenols attenuate A $\beta$  oligomer-induced intracellular ROS primarily via their antioxidant properties rather than by altering oligomer size and/or conformation. However, the dual-mechanism treatment with KAE was able to decrease A $\beta$  oligomer-induced intercellular ROS significantly more than when acting though antioxidant capability alone, demonstrating potential synergy between the two mechanisms for this polyphenol.

### *3.3.6 Polyphenols reduce A $\beta$ oligomer-induced caspase activation*

The roles of polyphenol modulation of oligomerization (Figures 3.2 and 3.3) and antioxidant activity (Figure 3.5 A) toward reducing A $\beta$  oligomer activation of caspases (Figure 3.4 B) were also examined. Cells treated for 24 h with 0.01  $\mu$ M A $\beta_{1-42}$  oligomers prepared in the presence of polyphenols, to isolate the role of polyphenol-modulated oligomerization, showed no change in caspase activation compared to cells treated with oligomers prepared alone (Figure 3.6 A, left panels; Figure 3.6 B, open bars). However, cells treated (24 h) simultaneously with 40  $\mu$ M polyphenol and 0.01  $\mu$ M A $\beta_{1-42}$  oligomers formed in the absence of polyphenol, to isolate antioxidant activity, displayed a >50% decrease in caspase activity when either LUT or QUE were included in treatments (Figure 3.6 A, middle panels; Figure 3.6B, closed bars). Furthermore, LUT and QUE were superior at decreasing A $\beta$  oligomer activation of caspases compared to FLA ( $p<0.05$  and  $p<0.01$ , respectively), API ( $p<0.05$  and  $p<0.01$ , respectively), and KAE ( $p<0.05$ ). Thus,

polyphenol attenuation of A $\beta$  oligomer-induced intracellular ROS through antioxidant capacity (Figure 3.5 B, closed bars) is paralleled by a reduction in oligomer-induced caspase activity, suggesting that A $\beta$ -mediated ROS second messengers may play a role in caspase activation.

Treatment of cells with 40  $\mu$ M polyphenol and 0.01  $\mu$ M A $\beta_{1-42}$  oligomers formed in the presence of polyphenol, to facilitate both mechanisms in concert, again resulted in a significant decrease in caspase activity when either LUT or QUE were included in treatments, while treatments including FLA or API failed to attenuate A $\beta$  oligomer activation of caspases (Figure 3.6 A right panel; Figure 3.6 B, grey bars). Similar to ROS reduction, these results parallel cellular treatments designed to isolate antioxidant capability, again indicating that attenuation of oligomer-induced cellular responses may be governed by polyphenol antioxidant capability. Interestingly, KAE again showed potential for synergy between the two mechanisms by significantly decreasing oligomer-induced caspase activity when treatments facilitated both mechanisms, despite being ineffective when either mechanism was isolated. In fact, within dual-mechanism treatments, KAE was superior to all other polyphenols (FLA, QUE p<0.05; API, LUT p<0.01).

### 3.4 Discussion

Epidemiological studies demonstrating that polyphenol-rich diets correlate with a reduced incidence of AD has made polyphenols promising candidates for natural AD therapeutics.<sup>47-49</sup> Additionally, the ability of polyphenols to intervene in the A $\beta$  aggregation pathway<sup>50,53,55,79,80</sup> and their ability to mitigate various diseases through their antioxidant capabilities,<sup>62-64</sup> gives polyphenols the potential to synergistically attenuate AD pathogenesis. The present study investigated the ability of polyphenols FLA, API,

LUT, KAE and QUE to reduce A $\beta$  oligomer-induced intracellular ROS and caspase activation by 1) altering oligomer formation and 2) acting as antioxidants. The ability of these two mechanism to synergistically reduce oligomer-induced cellular responses was also explored. These investigations identified that while the studied polyphenols primarily reduce oligomer-induced cellular responses through their antioxidant capabilities, KAE is able to synergistically attenuate oligomer-induced cellular responses.

The effect A $\beta$  oligomers have on cellular responses was investigated by evaluating changes to intracellular ROS and caspase activation. A $\beta_{1-42}$  oligomers at a concentration of 0.01  $\mu$ M were found to increase intracellular ROS in SH-SY5Y cells by a 1.4 fold increase, a similar increase to that observed for treatment with 25  $\mu$ M H<sub>2</sub>O<sub>2</sub> (Figure 3.4 A). Oligomers were also shown to significantly increase caspase activity (Figure 3.4 C) which regulates vital cell networks responsible for inflammation and apoptosis.<sup>38</sup> These results support previous findings that A $\beta$  aggregates increase both ROS and caspase activation.<sup>97-</sup><sup>101</sup> Since the upregulation of ROS has been implicated in various neurodegenerative diseases<sup>82</sup> and caspase activation has been shown to further the pathology of AD by stimulating apoptosis, inducing tau cleavage, promoting tau tangle formulation, and cleaving APP,<sup>82,102</sup> these observations suggest that attenuating oligomer-induced intracellular ROS and caspase activation could be a key therapeutic strategy for AD treatment.

All polyphenols tested exhibited high antioxidant capacity (Figure 3.5 A), paralleling with previous studies investigating polyphenols as antioxidants.<sup>103-106</sup> This antioxidant strength translated to an exceptional attenuation of oligomer-induced cellular responses, with all polyphenols significantly reducing A $\beta$  oligomer-induced intracellular

ROS (Figure 3.5 B, closed bars). Additionally, LUT and QUE were able to reduce oligomer-induced caspase activation through their antioxidant capabilities (Figure 3.6 B, closed bars). The superiority of LUT and QUE over the other polyphenols tested is likely due to their 3',4' catechol structure, which has been suggested as a key structural element for cellular protection by polyphenols.<sup>107</sup> For all polyphenols except KAE, the reduction of oligomer-induced cellular responses when both mechanisms of action were used was similar to the reduction observed when only the polyphenols' antioxidant activity was employed (Figures 3.5 B and 3.6 B), indicating these polyphenols predominately reduce oligomer-induced cellular responses through their antioxidant capabilities instead of by altering oligomer formation. This finding correlates with other studies that have suggested antioxidant capability is the primary mechanism by which polyphenols rescue cells from A $\beta$  cytotoxicity.<sup>44,108</sup>

Despite all hydroxylated polyphenols significantly altering oligomer formation (Figure 3.2 B-C and Figure 3.3), only LUT-induced changes to oligomers resulted in a reduction of intracellular ROS (Figure 3.5 B, open bars) and oligomer-induced caspase activation remained unchanged by oligomer alterations (Figure 3.6 B, open bars). While LUT was inferior to the other hydroxylated polyphenols at altering oligomer size distribution, it was the only polyphenol capable of reducing oligomer surface hydrophobicity. Increased oligomer surface hydrophobicity has been suggested as a primary governing factor in oligomer toxicity<sup>109–111</sup> and computational models have indicated that increased surface hydrophobicity promotes the insertion of oligomers into the cell membrane.<sup>110</sup> Combined, these results suggest that modulating the oligomer conformation by reducing surface hydrophobicity may be more effective at attenuating

oligomer-induced cellular responses than by altering oligomer size distribution. Contrastingly, previous studies have shown that polyphenol-induced changes to A $\beta$  aggregates can greatly effect aggregate cellular responses. Fibrils made in the presence of myricetin showed attenuation of MTT reduction in HEK 293 cells<sup>80</sup> and multiple flavonoids attenuated MTT reduction in PC12 cells by altering fibril formation.<sup>104</sup> This conflicting data could imply that other polyphenols have a greater potential at reducing oligomer-induced cellular responses or that polyphenols are more effective at reducing A $\beta$  aggregate-induced responses by altering fibril formation rather than by altering oligomer formation. Alternatively, the reduction in toxicity observed by these studies may be partially due to other neuroprotective effects, such as antioxidant capability, as the final cell treatment of polyphenol in these studies ranged from 1–50  $\mu$ M. These neuroprotective effects are much less likely to occur in the present study because of the low final treatment concentration of polyphenol (0.1  $\mu$ M).

KAE was the only polyphenol tested that was able to synergistically reduce oligomer-induced cellular responses despite having no impact when only altering oligomer formation and being unable to reduce caspase activation through antioxidant capabilities alone (Figure 3.5 B and 6 B). While the exact mechanism was not investigated, KAE has been shown to protect against A $\beta$ -induced toxicity in SH-SY5Y cells.<sup>112</sup> Additionally, KAE's antioxidant and anti-aggregation capabilities led to a reduction of A $\beta$ -induced cytotoxicity in PC12 cells.<sup>104</sup> These findings demonstrate the potential of KAE as a therapeutic for AD by synergistically attenuating oligomer-induced cellular responses.

Among the observed alterations to oligomer formation, key structural elements were identified that allow polyphenols to alter oligomer size distribution. FLA was the

only polyphenol tested unable to reduce the amount of larger oligomers formed (Figure 3.2 A-C) and was also unable to alter oligomer conformation (Figure 3.3), indicating the importance of polyphenol hydroxylation for oligomer alteration. KAE and QUE were found to be superior to API and LUT at altering oligomer size distribution (Figure 3.2 B), demonstrating the importance of a hydroxyl group at the 3 position. However, a hydroxyl at the 3' position was found to be less crucial, with LUT and QUE displaying no increase in oligomer inhibition compared to API and KAE. Previous studies have concluded that a 4' hydroxyl group on the polyphenols fisetin and 3, 3', 4', 5, 5'-pentahydroxyflavone is key to their ability to inhibit A $\beta$  fibril formation.<sup>113,114</sup> All polyphenols in this study except FLA contained a 4' hydroxyl group, suggesting this hydroxyl group may be a key factor to oligomer inhibition as well. These same studies also cited the 3' hydroxyl group as being crucial for A $\beta$  fibril inhibition. However, this hydroxyl group was found to not significantly improve oligomer inhibition, suggesting that the optimum polyphenol structure for altering oligomer and fibril formation may be different.

The reduction to monomer, trimer, and tetramer A $\beta$  species by polyphenols (Figure 3.2 D-G) suggests that the polyphenols are not directly interacting with these smaller A $\beta$  species to prevent the formation of larger oligomers but instead are shifting the oligomer size distribution towards larger aggregates. Other studies have shown that various polyphenols can only interact or bind with A $\beta$  aggregates once the aggregates have acquired a certain structure.<sup>54,83,115</sup> These studies along with the polyphenol-induced changes observed for 25-250 kDa oligomers support the idea that polyphenols are more effective at interacting with larger A $\beta$  oligomers than A $\beta$  monomer, trimer and tetramer species.

Through a combination of biophysical and cellular assays, this study has determined the ability of five polyphenols to attenuate oligomer-induced cellular responses. All polyphenols displayed excellent antioxidant capabilities, which resulted in a significant reduction in oligomer-induced intracellular ROS. For LUT and QUE, their antioxidant capabilities were additionally able to reduce A $\beta$  oligomer-induced caspase activation. While LUT was also able to reduce oligomer-induced intracellular ROS by alerting oligomer formation, this compound along with FLA, API, and QUE primarily attenuated oligomer-induced cellular responses through their antioxidant capabilities. Interestingly, KAE demonstrated the ability to synergistically reduce both ROS and caspase activation when both mechanisms of action worked in concert despite having little effect when the mechanisms were used separately. Together, these findings identify several promising polyphenols as natural therapeutics for AD and provide insight into their mechanism of action.

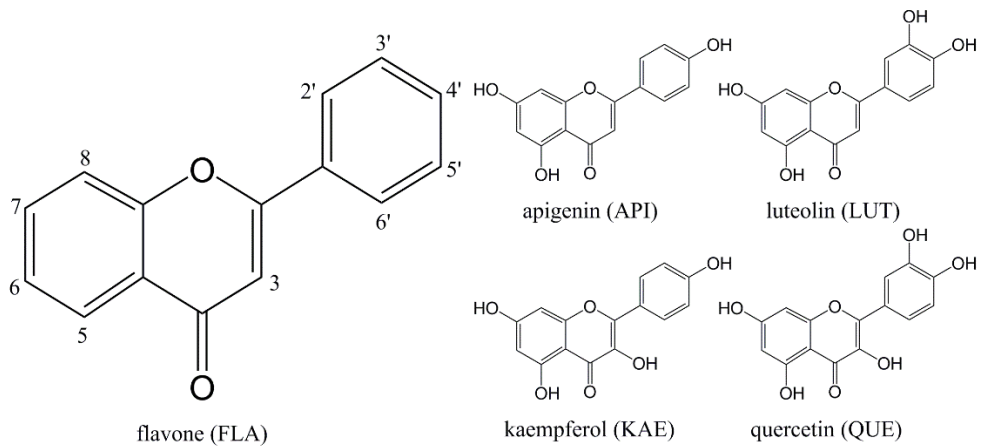


**Figure 3.1 Polyphenol structures.** Structures of flavone (FLA), apigenin (API), luteolin (LUT), kaempferol (KAE), and quercetin (QUE), which were evaluated for their ability to disrupt A $\beta$  oligomerization and cellular activity.

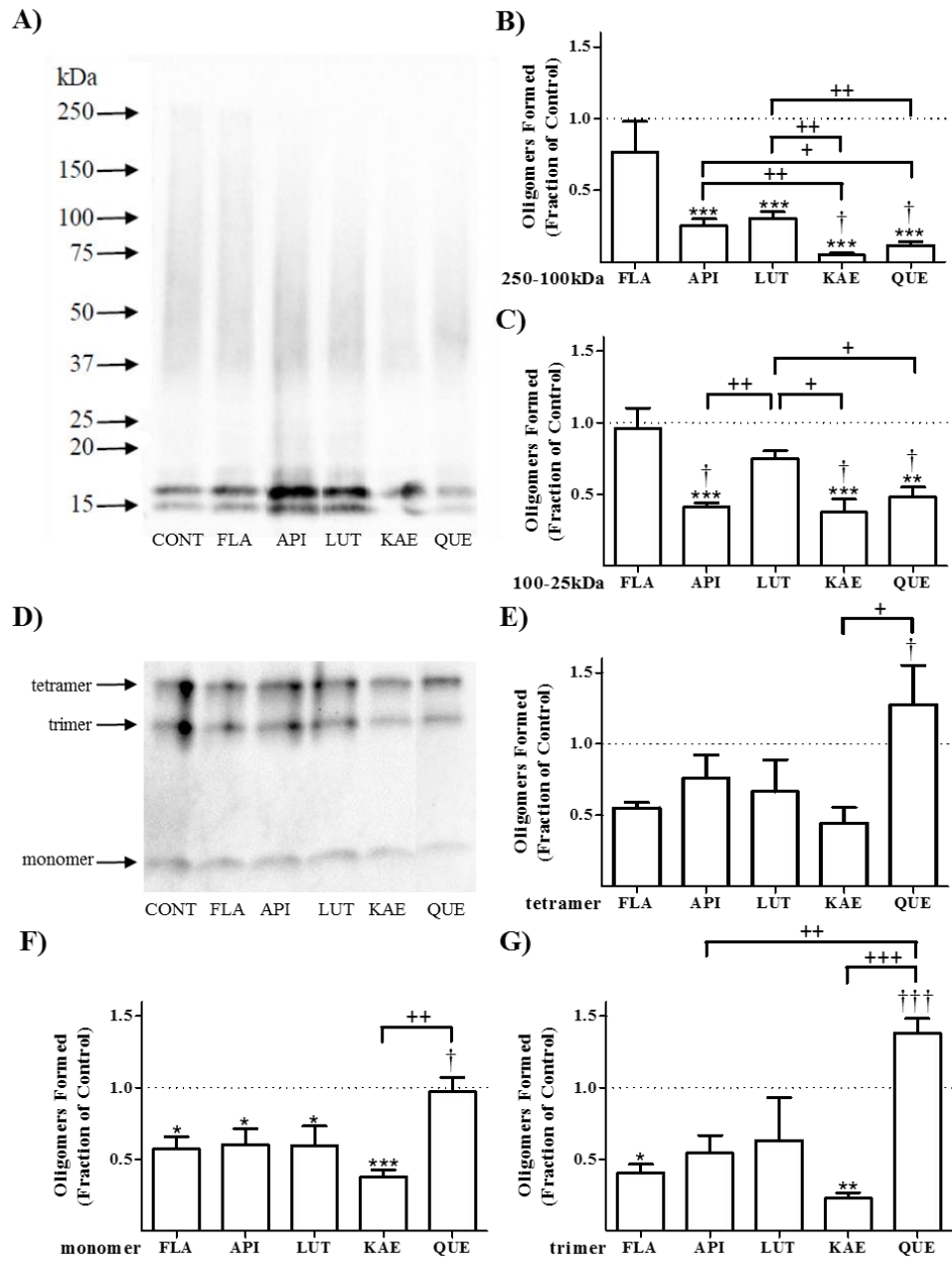


**Figure 3.2 Polyphenols alter A $\beta$  oligomer size distribution.** A $\beta$  oligomers were prepared in the absence (control, CONT) or presence of polyphenols flavone (FLA), apigenin (API), luteolin (LUT), kaempferol (KAE), or quercetin (QUE). Briefly, A $\beta$  monomer was combined with polyphenol in DMSO, and oligomerization was initiated via dilution into phosphate buffer containing 1  $\mu$ M NaCl, for final concentrations of 15  $\mu$ M A $\beta$ , 150  $\mu$ M polyphenol, and 2.5% DMSO. Reactions were incubated for 30 min at 25 °C then stabilized via addition of Tween (0.1%). Resulting oligomer products were resolved by SDS-PAGE on either a 4-20% Tris-glycine gel (panel A) or

a 16.5% Tris-tricine gel (panel D), transferred to nitrocellulose membrane, and probed with 6E10 antibody. Images are representative of 3-5 independent experiments. Using volumetric analysis in conjunction with the 4-20% Tris-glycine gel images (panel A), oligomer species within size ranges of 250-100 kDa (panel B) and 100-25 kDa (panel C) were quantified. Using band intensity analysis in conjunction with the 16.5% Tris-tricine gel images (panel D), tetramer (panel E), trimer (panel F) and monomer (panel G) species were quantified. Reported results are normalized to control, indicated by the dashed line with a value of 1 and representing no change. Error bars indicate SEM, n=3-5. \* $p<0.05$ , \*\* $p<0.01$ , and \*\*\* $p<0.001$  versus control; † $p<0.05$  and ††† $p<0.001$  versus flavone; + $p<0.05$ , ++ $p<0.01$ , and +++ $p<0.001$  between samples.

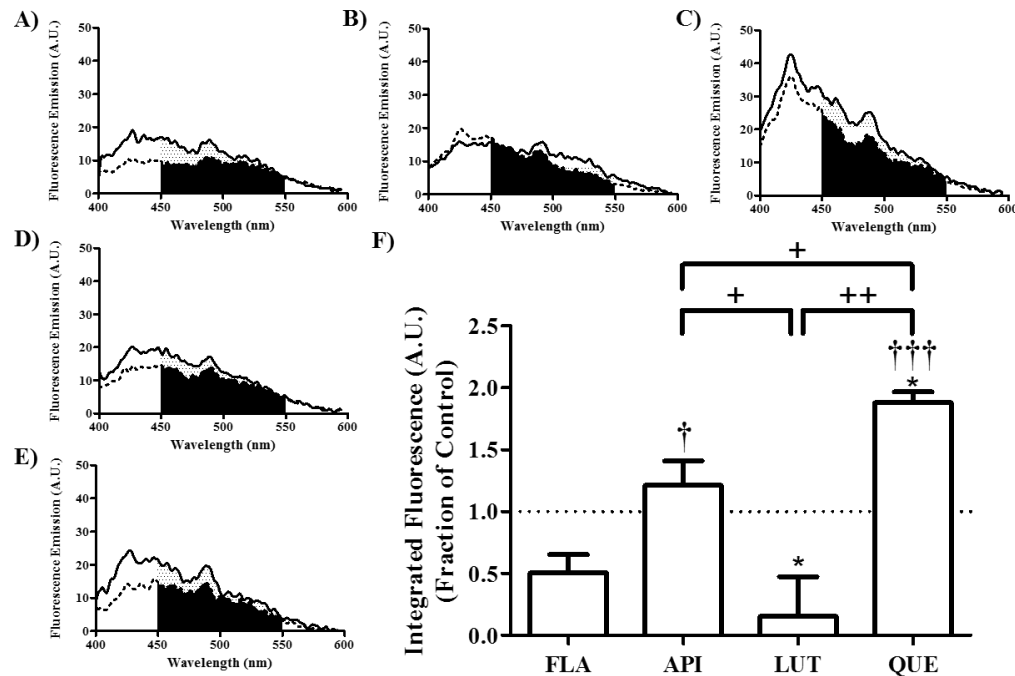


**Figure 3.3 Polyphenols alter A $\beta$  oligomer surface hydrophobicity.** A $\beta$  oligomers were prepared in the absence (CONT, panel A) or presence of polyphenols flavone (FLA, panel B), apigenin (API, panel C), luteolin (LUT, panel D), or quercetin (QUE, panel E) as described in Figure 3.2. Resulting oligomer products were diluted in ANS solution for final concentrations of 1  $\mu$ M A $\beta$ <sub>1-42</sub>, 10  $\mu$ M polyphenol, and 100  $\mu$ M ANS. Fluorescence emission was measured from 400-600 nm with excitation at 350 nm (panels A-E). Solid line indicates sample reading, and dashed line indicates blank reading (buffer or polyphenol with ANS). F) Fluorescence values were determined as the IAUC from 450-550 nm, corrected by blank subtraction. Corrected fluorescence was normalized to the control, indicated by the dashed line with a value of 1 and representing no change. Error bars indicate SEM, n=3-4. \* p<0.05 versus control; † p<0.05 and ‡ p<0.001 versus flavone; + p<0.05 and ++ p<0.01 between samples.

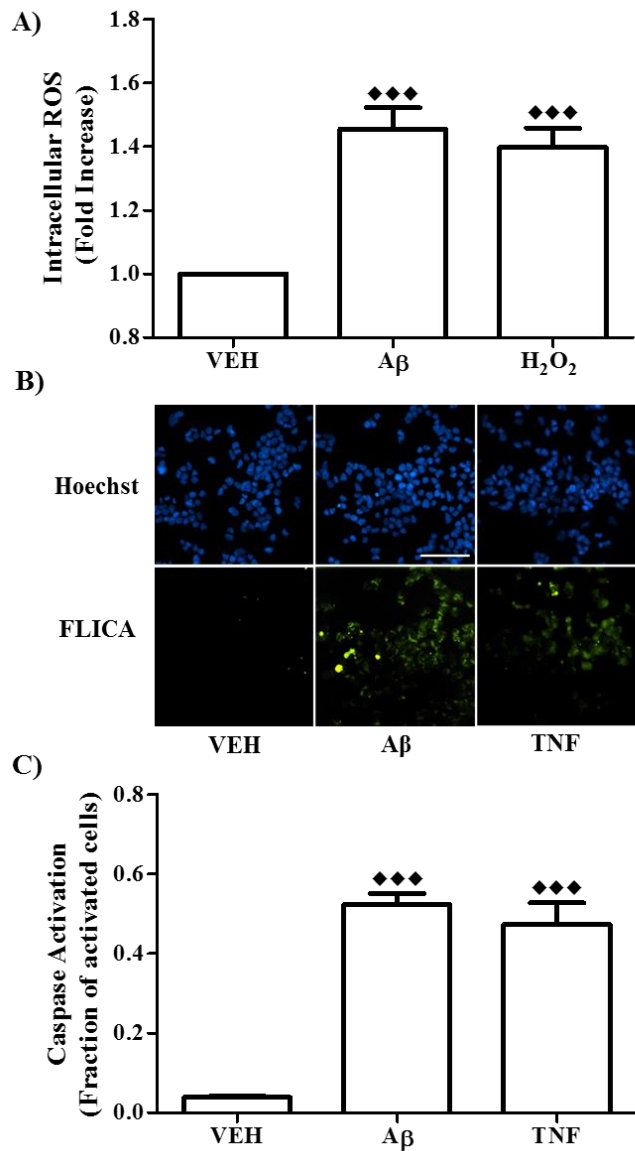


**Figure 3.4  $\text{A}\beta$  oligomers increase intracellular ROS and caspase activation in human neuroblastoma cells.** SH-SY5Y cells were incubated for 24 h with buffer equivalent (vehicle, VEH) or 0.01  $\mu\text{M}$   $\text{A}\beta$  oligomers ( $\text{A}\beta$ ). A) Intracellular ROS was evaluated using the DCFH-DA probe, as described in Section 2.8. Treatment with 25  $\mu\text{M}$   $\text{H}_2\text{O}_2$  served as positive control. Results are expressed as the fold-increase in intracellular ROS relative to the vehicle. Error bars indicate SEM,  $n=14$ . B) Caspase activation was evaluated via staining with FLICA reagent for detection of caspase-1, -3, -4, -5, -6, -7, -8 and -9 (green) in

conjunction with nuclear (Hoechst) staining (blue). Treatment with 1.5 U/ $\mu$ L TNF- $\alpha$  served as positive control. Scale bar represents 50  $\mu$ m. Images are representative of 8-13 independent experiments. C) Using custom MATLAB functions, cellular caspase activation was determined from Hoechst and FLICA images to quantify the total number of cells and the number of caspase activated cells, respectively, as described in Section 3.3. Results are reported as the fraction of caspase activated cells. Error bars indicate SEM, n=8-13. \*\*\*p<0.001 vs. vehicle.

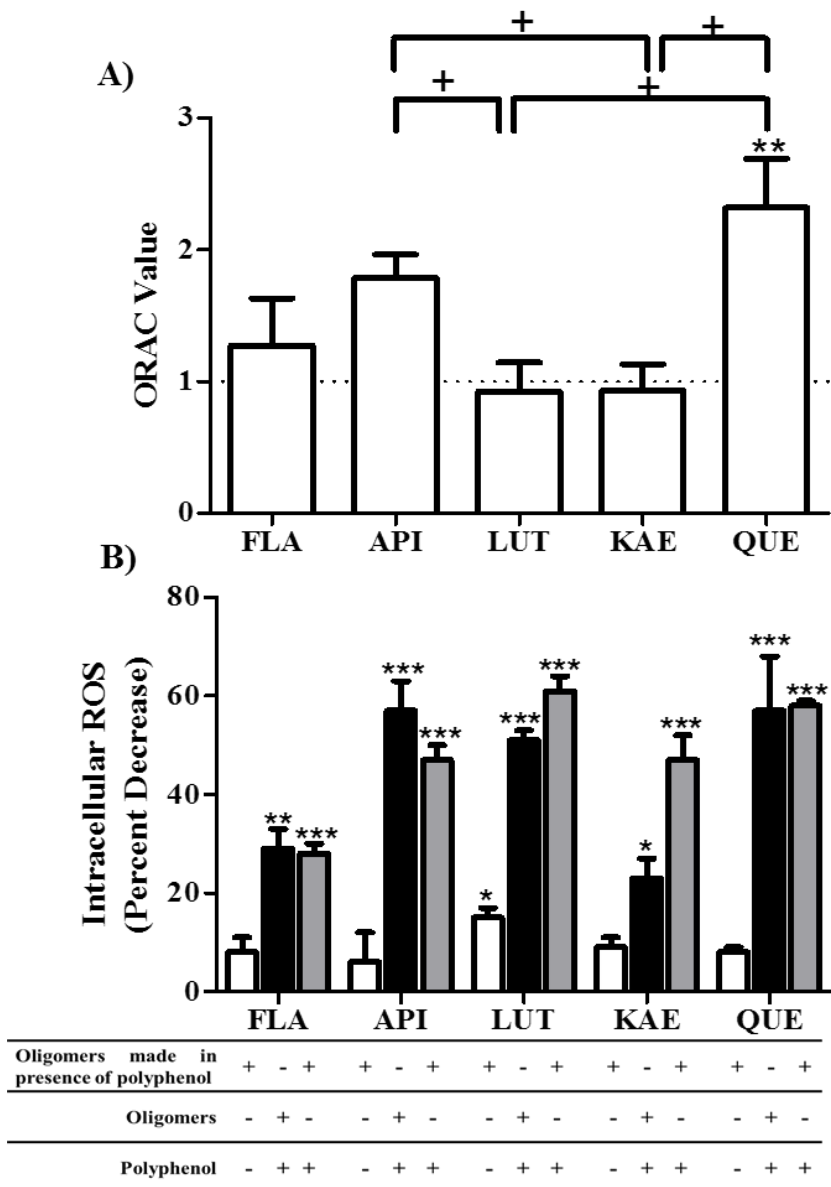


**Figure 3.5 Polyphenols possess potent antioxidant capability and reduce A $\beta$  oligomer-induced intracellular ROS**

A) Polyphenols flavone (FLA), apigenin (API), luteolin (LUT), kaempferol (KAE), and quercetin (QUE) were diluted in 75 mM phosphate (pH 7.0) and subjected to an ORAC assay alongside a Trolox standard as described in Section 2.6. ORAC values are expressed as the equivalent Trolox concentration per molar concentration of polyphenol. ORAC value of Trolox is indicated by the dashed line. Error bars indicate SEM, n=3-4. \*\*p<0.01 versus Trolox; +p<0.05 between samples.

B) SH-SY5Y cells were incubated for 24 h with or without 40  $\mu$ M polyphenol and

with 0.01  $\mu$ M A $\beta$  oligomers formed in either the presence or absence of polyphenols as indicated. Treatments were designed to isolate mechanisms for polyphenol attenuation of ROS: modulation of oligomer formation (open bars), antioxidant action (closed bars), or both mechanisms in concert (grey bars). Intracellular ROS was evaluated using the DCFH-DA probe, as described in Section 3.2.6. Results are expressed as the percent decrease in intracellular ROS relative to treatment with A $\beta$  oligomers alone. Error bars indicate SEM, n=3-4. \*p<0.05, \*\*p<0.01, and \*\*\*p<0.01 vs. A $\beta$  oligomers alone.

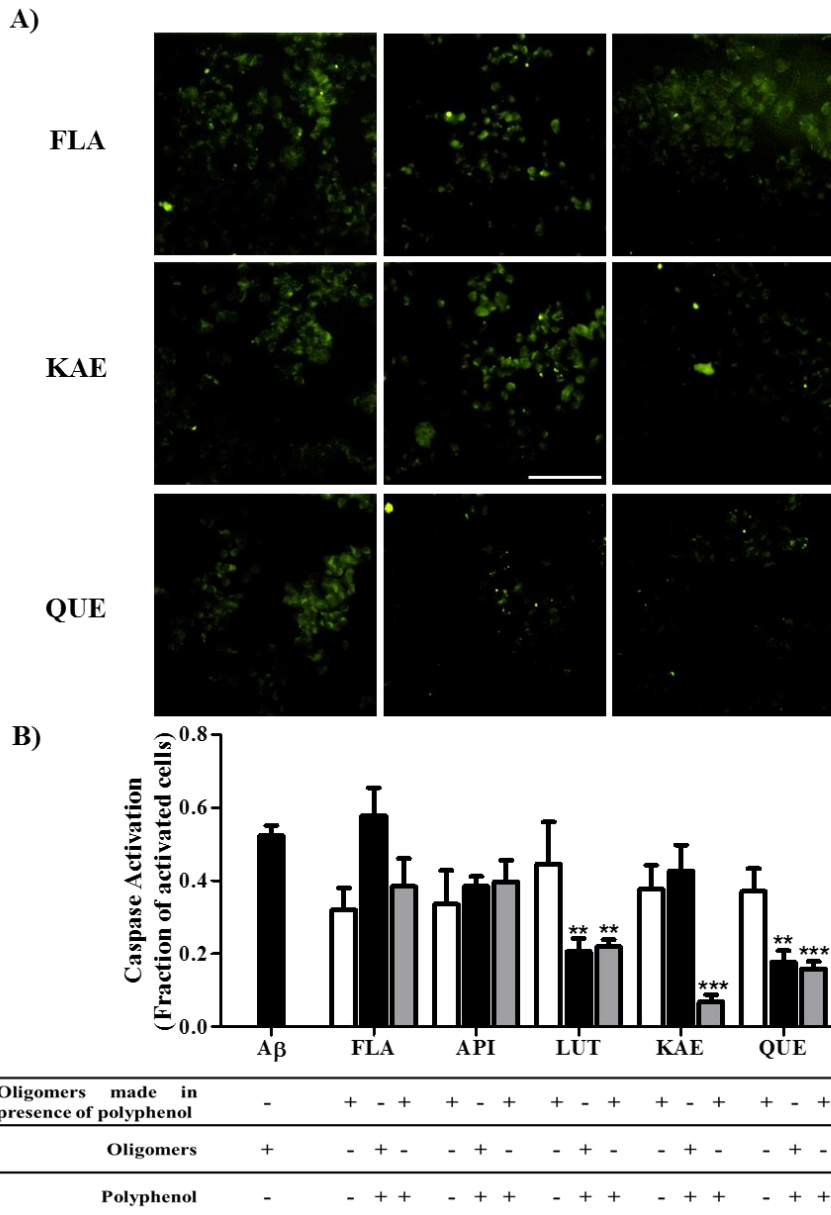


**Figure 3.6 Polyphenols reduce A $\beta$ -induced caspase activation.**  
 A) SH-SY5Y cells were treated for 24 h with indicated treatments of A $\beta$  oligomers and 40  $\mu$ M flavone (FLA), apigenin (API), luteolin (LUT), kaempferol (KAE), or quercetin (QUE) as described in Figure 3.5. Caspase activation was evaluated via staining with FLICA reagent for detection of caspase-1, -3, -4, -5, -6, -7, -8 and -9. Scale bar represents 50  $\mu$ m. Images are representative of 3-4 independent experiments. Additional images for remaining polyphenols and coinciding Hoechst images can be found in Appendix C. B) Cellular caspase activation was determined from Hoechst and FLICA images as described in Figure 3.4 to isolate mechanisms for polyphenol attenuation of caspase activation:

modulation of oligomer formation (A left column, B open bars), antioxidant action (A middle column, B closed bars), or both mechanisms (A right column, B grey bars). Results are reported as the fraction of caspase activated cells. Error bars indicate SEM, n=3-5. \*\*p<0.01 and \*\*\*p<0.001 versus A $\beta$  oligomers alone.

## CHAPTER 4

### QUERCETIN METABOLITES ARE EQUALLY AS EFFECTIVE AS QUERCETIN AT ATTENUATING A $\beta$ OLIGOMER-INDUCED CELLULAR RESPONSES

#### 4.1 Introduction

Antioxidants have long been known to exert numerous health benefits and have been studied as possible therapeutics for a host of diseases.<sup>33,116–119</sup> As mentioned in Section 1.3, some of the most studied antioxidants are polyphenols due to epidemiological studies supporting the health benefits from high polyphenol intake.<sup>47,48,120–123</sup> QUE, one of the polyphenols studied in Chapter 3, is the main polyphenol in the human diet<sup>124,125</sup> and has demonstrated promise as a natural therapeutic for a variety of ailments including cardiovascular disease, cancer, neurodegenerative disease, and diabetes.<sup>33,121,123,126</sup> However, since QUE is readily metabolized in the liver and intestines leaving very little free QUE, scientist now believe many of the health benefits attributed to oral administration of QUE could actually be attributed to its metabolites.<sup>126–129</sup> In fact, studies have shown that QUE metabolites have greater accumulation than QUE due to slower elimination from the body<sup>128,130</sup> and that these metabolites exhibit similar or greater protective effects.<sup>126,131</sup> Due to the evidence supporting the therapeutic properties of both QUE and its metabolites, this study sought to compare the therapeutic potential of QUE and three of its most common metabolites, rhamnetin (RHA), isorhamnetin, (IRHA), and tamarixetin (TAM), in relation to AD (Figure 4.1).

Polyphenols, including QUE, have been of interest as natural therapeutics for AD due to their ability to reduce ROS via their antioxidant capabilities. Oxidative stress caused by the overproduction of ROS is believed to play a key role in the pathology of AD.<sup>33,47,82,132</sup> The primary cause of the increase in ROS is the aggregation of the amyloid- $\beta$  (A $\beta$ ) protein associated with AD pathology. A $\beta$  aggregates have been proven to produce both H<sub>2</sub>O<sub>2</sub> and free radicals; furthermore, a positive feedback loop has been suggested with A $\beta$  aggregate-induced oxidative stress leading to the production of more A $\beta$  aggregates.<sup>33,133,134</sup> Studies have shown the ability of polyphenols and specifically QUE to attenuate the increased ROS created by A $\beta$  aggregates.<sup>33,68,69</sup> While the results of QUE are promising, there has been little investigation into the ability of QUE metabolites to reduce A $\beta$  aggregate-induced ROS.

The antioxidant strength that polyphenols possess are not the only attribute that make them promising therapeutics for AD. As mentioned in Section 1.3, polyphenols have also demonstrated the ability to intervene in the A $\beta$  aggregation pathway resulting in fewer aggregates being formed, aggregates of altered size and conformation, and, most notably, aggregates with reduced cytotoxicity.<sup>54,68–70,113,114</sup> While QUE has been studied for its ability to inhibit the formation of A $\beta$  fibrils,<sup>68–70</sup> data is lacking on the ability of QUE and its metabolites to alter the formation of A $\beta$  oligomers, the most toxic A $\beta$  aggregate species,<sup>23–25,135</sup> and if these alterations can attenuate oligomer-induced cellular responses.

This chapter investigated the ability of QUE, RHA, IRHA, and TAM to attenuate A $\beta$  oligomer-induced cellular responses through two separate mechanisms: their antioxidant capability and their ability to alter oligomer formation. Additionally, the potential of these polyphenols to serve as dual-action therapeutics by acting through both

mechanisms was determined. Due to the antioxidant nature of polyphenols and the key role ROS is believed to play in AD pathology, the ability of polyphenols to reduce A $\beta$  oligomer-induced intracellular ROS was investigated. Additionally, the ability of polyphenols to reduce A $\beta$  oligomer-induced caspase activation was determined since intracellular ROS is known to trigger caspase activation<sup>136–139</sup> and since caspase activation has demonstrated the ability to further AD pathology by inducing apoptosis, cleaving APP, inducing tau cleavage, and promoting tau tangle formation.<sup>82,102</sup>

Investigations revealed that not only can QUE reduce A $\beta$  oligomer-induced cellular responses but that its metabolites are just as effective at doing so. Results further showed that polyphenols attenuate A $\beta$  oligomer-induced cellular responses through different mechanisms, with QUE and TAM primarily acting via their antioxidant properties while IRHA is more effective when altering oligomer formation. Notably, RHA is equally effective at reducing oligomer-induced cellular responses regardless of which mechanism is employed. These results support the idea that QUE is not solely responsible for the attenuation of AD pathology but, that many of the therapeutic effects attributed to it are a result of QUE metabolites.

## 4.2 Materials and Methods

### 4.2.1 Preparation of Polyphenols

Polyphenols QUE, RHA, and IRHA were purchased from Sigma Aldrich (St. Louis, MO) and TAM was purchased from Fisher Scientific (Waltham, MA). All polyphenols were freshly dissolved in DMSO to a concentration of 10mM to be used in experiments.

#### *4.2.2 Assessment of Polyphenol Antioxidant Capacity via ORAC Assay*

Antioxidant capacities of polyphenols were assessed using the ORAC assay as described in Section 2.6. Results are reported as the ORAC value, which is the equivalent Trolox concentration per unit concentration of polyphenol.

#### *4.2.3 Preparation of A<sub>β</sub><sub>1-42</sub> Oligomers*

A<sub>β</sub><sub>1-42</sub> oligomers were formed in the absence (control) or presence of a 10-fold excess of either QUE, RHA, IRHA, or TAM as described in Section 2.2.

#### *4.2.4 Determination of A<sub>β</sub><sub>1-42</sub> Oligomer Size via SDS-PAGE and Western blot*

To determine whether polyphenols present during oligomerization alter oligomer size distribution, SDS-PAGE with Western blotting was performed as described in Section 2.3. Image Lab software was used for quantification of both larger (250 kDa – 100 kDa) and smaller (100 kDa – 25 kDa) oligomers as well as monomer, trimer, and tetramer species. Intensity values for each range are reported as a fraction of the control.

#### *4.2.5 Assessment of A<sub>β</sub><sub>1-42</sub> Oligomer Conformation via ANS and Nile Red Spectroscopy*

Nile Red was used as described in Section 2.5 to determine if polyphenols could alter oligomer conformation when present during oligomerization. Nile Red emits an increased fluorescent intensity with a blue shift when in the presence of exposed non-polar molecular surfaces. A LS-45 luminescence spectrophotometer (Perkin Elmer, Waltham, MA) was used to measure the fluorescence (excitation = 550 nm, emission = 580 – 700 nm) and the IAUC was calculated with blank (Nile Red plus buffer or polyphenol) subtraction.

Upon examination of blank readings, it was discovered that QUE interferes with the fluorescent signal of Nile Red, therefore ANS was used as an alternative for this

compound. ANS experiments were performed as described in Section 2.4 and fluorescence values were determined as the IAUC from 450-550 nm with blank subtraction. Results for both Nile Red and ANS are reported as a fraction of the control.

#### *4.2.6 Cell Culture and Treatment*

SH-SY5Y cells were maintained as described in Section 2.7. To determine the ability of strong antioxidants to attenuate A $\beta$ <sub>1-42</sub> oligomer-induced cellular responses, cells were simultaneously treated with 0.01  $\mu$ M A $\beta$ <sub>1-42</sub> oligomers and 10  $\mu$ M polyphenol diluted in media. This lower concentration of polyphenol was used rather than the 40  $\mu$ M used in Chapter 3 due to some of QUE's metabolites causing increased cellular responses at the higher concentration. To explore the potential of polyphenols to reduce A $\beta$ <sub>1-42</sub> oligomer-induced cellular responses by altering oligomer formation, rather than through their antioxidant properties, cell were treated with A $\beta$ <sub>1-42</sub> oligomers formed in the presence or absence (control) of polyphenols and diluted in media to final concentrations of 0.01  $\mu$ M A $\beta$ <sub>1-42</sub> oligomers and 0.1  $\mu$ M polyphenol. Additionally, cells were treated with 0.01  $\mu$ M A $\beta$ <sub>1-42</sub> oligomers formed in the presence of polyphenol plus 10  $\mu$ M polyphenol to determine the potential of polyphenols to serve as dual-action therapeutics by reducing A $\beta$ <sub>1-42</sub> oligomer-induced cellular responses via both mechanisms (antioxidant capability and altering oligomer formation).

#### *4.2.7 Evaluation of Antioxidants Ability to Reduce A $\beta$ <sub>1-42</sub> Oligomer-Induced Intracellular ROS*

An OxiSelect™ intracellular ROS assay kit was implemented as described in Section 2.8 to assess the ability of polyphenols to reduce oligomer-induced intracellular ROS. Cells were exposed to varying treatments of A $\beta$ <sub>1-42</sub> oligomers and polyphenol diluted

in phenol red free media containing 1% FBS as described in Section 4.2.6. Resulting fluorescent values were blank subtracted and converted to DCF concentration using a DCF standard curve. Results are reported as the intracellular ROS as fraction of negative control.

#### *4.2.8 Evaluation of A $\beta$ <sub>1-42</sub> Oligomer-Induced Caspase Activation*

The Image-iT LIVE Green Poly Caspases detection kit was used as described in Section 2.9 to determine the ability of polyphenols to attenuate A $\beta$ <sub>1-42</sub> oligomer-induced caspase activation. Cells were exposed to varying treatments of A $\beta$ <sub>1-42</sub> oligomers and polyphenol diluted in media containing 1% FBS media as described in Section 4.2.6. Results are expressed as the fraction (FLICA/Hoechst) of caspase activated cells.

### **4.3 Results**

#### *4.3.1 Antioxidant capability of polyphenols result in reduced A $\beta$ oligomer-induced cellular responses*

An ORAC assay was used to assess the antioxidant strength of the compounds. All compounds exhibited similar antioxidant capability to that of the Trolox standard (Figure 4.2 A). While replacing the hydroxyl group with a methoxy group on the fused ring (transitioning from QUE to RHA) did not affect antioxidant strength, replacing hydroxyl groups on the attached ring to form IRHA and TAM did result in a loss in antioxidant strength, indicating that hydroxyls on the attached ring are more crucial for antioxidant capability.

The ability of polyphenols to reduce A $\beta$  oligomer-induced cellular responses via antioxidant capability was assessed in SH-SY5Y human neuroblastoma cells using a DCFH-DA probe and an Image-iT LIVE Green Poly Caspases detection kit to monitor

intracellular ROS and caspase activation, respectively. Cells treated with buffer or 10 µM polyphenol alone demonstrated that the concentrations of buffer and polyphenol used did not alter basal ROS and caspase levels (data not shown). As demonstrated in Section 3.3.3, A $\beta$  oligomers stimulate an increase in intracellular ROS in SH-SY5Y cells compared to cell treatment of buffer alone (Figure 4.2 B, p<0.001). In fact, the response in intracellular ROS was slightly greater for 0.01 µM A $\beta$  oligomers than for the positive control (25 µM H<sub>2</sub>O<sub>2</sub>). Simultaneous cell treatment with 0.01 µM A $\beta$  oligomers and 10 µM of either QUE, RHA, or IRHA showed a significant decrease in intracellular ROS compared to cells treated with A $\beta$  oligomers alone (Figure 4.2 B). TAM, however, failed to significantly impact the oligomers' effect on ROS. Paralleling with their antioxidant strength, QUE and RHA had the greatest effect on decreasing A $\beta$  oligomer-induced ROS, with both compounds reducing intracellular ROS significantly more than IRHA and TAM.

As demonstrated in Section 3.3.3, A $\beta$  oligomers also increase caspase activation in SH-SY5Y cells compared to buffer alone (Figure 4.2 C-E, p<0.001). This increase is similar to that observed for cells treated with the positive control (1.5 U/ $\mu$ L TNF- $\alpha$ ), demonstrating the potency of A $\beta$  oligomers on cellular responses. Analogous with their ability to reduce intracellular ROS, QUE and RHA were able to significantly reduce oligomer-induced caspase activation (Figure 2 C and E) thus demonstrating the ability of strong antioxidants to attenuate multiple A $\beta$ -induced cellular responses. Interestingly, TAM, the weakest antioxidant, significantly reduced oligomer-induced caspase activation even though it had no effect on intracellular ROS, indicating that it may be acting through alternative mechanisms.

#### *4.3.2 Both QUE and metabolites alter A $\beta$ oligomer size distribution and increase oligomer surface hydrophobicity*

A $\beta$  oligomers were formed in the absence (control) or presence of 10-fold excess of each polyphenol to evaluate alterations in oligomer size distribution and conformation. Resulting oligomers were evaluated using SDS-PAGE and Western blot for size distribution analysis (Figure 4.3 A-B). The quantity of oligomers formed in size ranges 250-100 kDa and 100-25 kDa was assessed (Figure 4.3 C-D) as well as the quantity of tetramer, trimer, and monomer species (Figure 4.3 E). QUE proved to be the most effect inhibitor of oligomers 250-100 kDa in size however, RHA and TAM also significantly reduced the quantity of oligomers in this size range (Figure 4.3 C). Meanwhile, IRHA failed to elicit any changes to the quantity of 250-100 kDa oligomers formed. All polyphenols significantly reduced the amount of 100-25 kDa oligomers formed, although IRHA was still inferior to all other polyphenols tested (Figure 4.3 D). The weak effect of IRHA in both size ranges indicates the presence of a hydroxyl group rather than a methoxy group on the 3' position is crucial for inhibition. Contrastingly, a methoxy substitution on both the 4' and 7 positions (TAM and RHA) still resulted in efficient reduction of oligomers within both size ranges, suggesting hydroxyl groups at these positions are less crucial for oligomer reduction.

The polyphenols had less of an impact on smaller A $\beta$  species. QUE and TAM did not significantly impact the quantity of monomer, trimer, or tetramer species while RHA and IRHA only reduced the amount of monomeric species (Figure 4.3 E). The lack of an increase in monomeric A $\beta$  when polyphenols are present indicates that the polyphenols are not directly binding to A $\beta$  monomer to stop aggregates from forming but instead interact

primarily with A $\beta$  oligomers. This interaction in turn effects the ability of A $\beta$  oligomers to bind to one another and/or A $\beta$  monomer, resulting in alterations in oligomer formation.

Oligomer conformational changes induced by the presence of the polyphenols were determined using either ANS or Nile Red. Both of these fluorescent dyes bind to hydrophobic residues on the surface of the oligomers resulting in an increased fluorescence. Due to QUE interference with Nile Red fluorescence, ANS was used to evaluate conformational changes caused by QUE. All polyphenols resulted in a significant increase in oligomer surface hydrophobicity compared to control oligomers (Figure 4.3 F). TAM resulted in the largest alteration, increasing oligomer surface hydrophobicity significantly more than QUE, RHA, and IRHA.

#### *4.3.3 Polyphenol-induced alterations to A $\beta$ oligomer formation result in reduced cellular responses*

The ability of compounds to reduce A $\beta$  oligomer-induced cellular responses by modifying oligomer formation was assessed using a DCFH-DA probe and an Image-iT LIVE Green Poly Caspases detection kit. Oligomers were formed in the presence of each compound and diluted to 0.01  $\mu$ M A $\beta$  and 0.1  $\mu$ M polyphenol in 1% FBS media. SH-SY5Y cells were treated with resulting oligomers for 24 h and compared against cells treated with control oligomers. Results demonstrate that only IRHA was able to significantly reduce A $\beta$ -induced intracellular ROS by altering oligomer formation (Figure 4.4 A). However, both RHA and IRHA were able to significantly reduce A $\beta$  oligomer-induced caspase activation, while QUE and TAM had no effect (Figure 4.4 B-C). These results prove that polyphenols can attenuate A $\beta$  oligomer-induced cellular responses not just through antioxidant capability but also by altering oligomer formation.

#### *4.3.4 Polyphenols attenuate A $\beta$ oligomer-induced cellular responses via different mechanisms but do not possess dual-action potential*

To determine if polyphenols possessed a dual-action ability to decrease A $\beta$  oligomer-induced cellular responses via two separate mechanisms (antioxidant capability and altering oligomer formation), cells were treated with 0.01  $\mu$ M A $\beta$  oligomers formed in the presence of polyphenol and an additional 10  $\mu$ M polyphenol. The ability of all polyphenols to decrease A $\beta$  oligomer-induced intracellular ROS was similar to the reduction observed when only antioxidant capability was utilized, with only QUE and RHA causing a significant reduction in intracellular ROS (Figure 4.5 A). This demonstrates that this set of polyphenols primarily attenuate oligomer-induced intracellular ROS via their antioxidant capability with minimal attenuation of ROS resulting from altering oligomer formation or dual-action attenuation.

All polyphenols were able to significantly decrease A $\beta$  oligomer-induced caspase activation when both mechanisms were utilized (Figure 4.5 B-C). Interestingly, the primary mechanism to achieve this decrease varies for each polyphenol. QUE and TAM only attenuate caspase activation when their antioxidant mechanism is employed, whereas IRHA acts solely through its ability to alter oligomer formation. RHA is the only compound that results in a significant reduction in caspase activation through the use of either mechanism. No increase in efficacy was observed for any polyphenol when both mechanisms were exerted compared to when only the polyphenol's dominate mechanism was used (either mechanism for RHA). This demonstrates that while all polyphenols can reduce A $\beta$  oligomer-induced caspase activation, these polyphenols do not possess dual-action potential.

#### 4.4 Discussion

Natural antioxidants, including polyphenols, have been of interest as possible therapeutics for a variety of ailments.<sup>33,116–119</sup> QUE is a widely studied polyphenol that has demonstrated potential for a host of therapeutic applications.<sup>33,121,123,126</sup> However, studies have suggested that it is not simply QUE but also its metabolites created upon oral administration that are the source of these health benefits.<sup>126,128,130,131</sup> This study investigated the ability of QUE and three of its most common metabolites (RHA, IRHA, and TAM) to attenuate A $\beta$  oligomer-induced cellular responses associated with AD. Investigations revealed these polyphenols can reduce A $\beta$  oligomer-induced intracellular ROS and caspase activation through two separate mechanisms: their antioxidant capability and by altering oligomer formation. Furthermore, studies showed that the primary mechanism by which the polyphenols attenuate A $\beta$  oligomer-induced cellular responses varies for each polyphenol.

All polyphenols studied were found to be strong antioxidants with antioxidant capability being similar or higher than the vitamin E analog, Trolox (Figure 4.2 A). Additionally, QUE and RHA were shown to significantly reduce oligomer-induced intracellular ROS via their antioxidant capability (Figure 4.2 B). These findings agree with previous studies that have shown QUE and RHA can protect against H<sub>2</sub>O<sub>2</sub>-induced oxidative damage<sup>140–142</sup> and that QUE can reduce A $\beta$  aggregate-induced ROS.<sup>143</sup> The inability of IRHA and TAM to reduce oligomer-induced intracellular ROS is likely due to these compounds not possessing the 3',4'-catechol structure on the attached ring that QUE and RHA possess. This catechol structure increases antioxidant capability, enhances inhibition of lipid peroxidation, and is a common structural element in the most potent ROS

and RNS scavengers.<sup>103,144–146</sup> On the other hand, IRHA has previously been shown to reduce H<sub>2</sub>O<sub>2</sub>-induced<sup>147</sup> and menadione-induced<sup>148</sup> ROS using cell pretreatment with higher doses of IRHA (25 -100 μM) for shorter exposure times (45 min – 4 h). However, for the purpose of investigating AD, a prolonged co-treatment with Aβ oligomers and low dose polyphenol is more therapeutically relevant.

Polyphenols QUE, RHA, and TAM were all effective inhibitors of Aβ oligomer-induced caspase activation (Figure 4.2 C). This parallels with the ability of QUE and RHA to reduce intracellular ROS which is known to trigger caspase activation.<sup>136–139</sup> However, since TAM was unable to attenuate oligomer-induced intracellular ROS, its ability to reduce caspase activation suggests that the antioxidant capacity of polyphenols can act through multiple mechanisms to attenuate oligomer-induced cellular responses. Antioxidants have been shown to reduce caspase activation by inhibiting the release of cytochrome c<sup>149</sup> and various polyphenols, including QUE, are believed to inhibit AP-1 activation and the JNK pathway, both of which stimulate caspase activation.<sup>150</sup> TAM is likely acting via one such mechanism to attenuate Aβ oligomer-induced caspase activation rather than by reducing ROS. Both QUE and TAM have been shown to decrease neuronal cell loss caused by oxidative damage<sup>151</sup> and to inhibit cholinesterases,<sup>152</sup> the reduction of which has been one therapeutic strategy for AD. Combined these studies support the findings that QUE, RHA, and TAM can attenuate Aβ oligomer-induced cellular responses.

The polyphenols investigated were found to modify Aβ oligomer formation by altering both the oligomer size distribution and conformation (Figure 4.3). QUE, RHA, and TAM all significantly reduced the amount of oligomers formed in both the 250-100 kDa and 100-25 kDa size ranges (Figure 4.3 C-D). IRHA had the weakest effect on

oligomers in both size ranges, completely failing to reduce oligomers 250-100 kDa in size. These results indicate that a methoxy group substitution on QUE at the 3' position (IRHA) drastically effects oligomer inhibitory capabilities, while a substitution at the 4' or 7 position (TAM and RHA) has little effect. Investigation of other polyphenol structures has likewise shown that the 3' hydroxyl is important for A $\beta$  aggregate inhibition, while a hydroxyl at the 7 position is not.<sup>113,114</sup> While the 4' hydroxyl group has also been identified as key for aggregate inhibition,<sup>113,114</sup> the inhibitory capability of TAM suggests that mere functionalization of the 4' position is satisfactory for effective aggregate inhibition. Although data is lacking on the effect these polyphenols have on oligomer aggregation, studies have shown that QUE and RHA, but not IRHA, inhibit A $\beta$  fibril formation<sup>70,114,153</sup> further supporting the current findings. The polyphenols had little effect on smaller A $\beta$  species (Figure 4.3 E) with only RHA and IRHA having any impact and only at reducing the amount of A $\beta$  monomer. Other studies have shown that various polyphenols can only interact or bind with A $\beta$  aggregates and not A $\beta$  monomer.<sup>54,83,115</sup> These results paired with the current findings that polyphenols can alter oligomer formation and previous studies demonstrating polyphenols alter fibril formation,<sup>70,113,114,153</sup> suggest that these polyphenols are more effective at interacting with A $\beta$  aggregates than A $\beta$  monomer.

All of the polyphenols significantly altered A $\beta$  oligomer conformation by increasing surface hydrophobicity (Figure 4.3 F). Some polyphenols have the ability to alter A $\beta$  fibril conformation by effecting the  $\beta$ -sheet structure.<sup>112,154,155</sup> This study shows the ability of polyphenols to act earlier on in the aggregation process by altering oligomer conformation. Substitution of a hydroxyl group with a methoxy group on QUE at either the 3' or 7 position (IRHA and RHA) had no effect on the resulting oligomer conformation

however, a substitution at the 4' position (TAM) further increased the surface hydrophobicity of the oligomers. While alterations to oligomer size distribution were determined by the 3' position of the polyphenol, alterations to oligomer conformation were dependent on the functionalization of the 4' position, highlighting the ability to modify different oligomer characteristics by altering polyphenol structure.

When testing the ability of polyphenols to attenuate oligomer-induced cellular responses by modifying oligomer formation, it was found that only IRHA had the ability to significantly reduce A $\beta$  oligomer-induced intracellular ROS (Figure 4.4 A). Interestingly this parallels with IRHA having the weakest effect on oligomer size distribution while still significantly altering oligomer conformation. A change in oligomer conformation has been shown to have drastic effects on toxicity even among oligomers of similar size,<sup>109,156,157</sup> indicating that changing the conformation, without shifting the size distribution, may be an effective approach to attenuate oligomer-induced responses. On the other hand, typically an increase in surface hydrophobicity has led to more toxic A $\beta$  aggregates,<sup>109,156,157</sup> suggesting the reduction in intracellular ROS observed may also involve another mechanism.

When present during oligomerization, RHA and IRHA were able to drastically reduce the amount of A $\beta$  oligomer-induced caspase activation (Figure 4.4 B-C). Since QUE produced similar alterations to oligomer size as RHA and since QUE, RHA, and IRHA all created oligomers with similar surface hydrophobicity, QUE not having a similar effect on caspase activation suggests that RHA and IRHA are acting via an additional mechanism. One such mechanism could be the inhibition of oligomer-cell interactions. It is believed that one contributing factor of AD pathology is the ability of A $\beta$  aggregates,

including oligomers, to interact with, bind to, and disrupt the cell membrane thereby triggering proinflammatory and proapoptotic pathways.<sup>158–162</sup> The interaction of methoxy groups with A $\beta$  oligomers, rather than just the hydroxyl groups present in QUE, may be altering the oligomers so that they are unable to interact with cell receptors. This has been observed with A $\beta$  aggregates formed in the presence of various inhibitors and has been proposed as a possible therapeutic strategy.<sup>163–165</sup> This would also further explain the ability of IRHA to reduce A $\beta$  oligomer-induced intracellular ROS when present during oligomer formation.

When each polyphenol was allowed to both exert antioxidant capabilities and alter oligomer formation, QUE and RHA successfully reduced oligomer-induced intracellular ROS (Figure 4.5 A). This reduction was similar to QUE and RHA's effect when only exerting their antioxidant capability, demonstrating that these polyphenols primarily reduce oligomer-intracellular ROS via antioxidant strength and do not possess dual-action potential. All polyphenols were able to attenuate A $\beta$  oligomer-induced caspase activation when acting via both mechanisms (Figure 4.5 B-C). While they did not exert dual-action potential, this study did reveal the primary mechanism by which each polyphenol reduces oligomer-induced caspase activation. QUE and TAM both primarily reduce caspase activation via their antioxidant properties while the reduction observed by IRHA stems from IRHA-induced alterations to oligomer formation. Interestingly, RHA is equally effective at reducing oligomer-induced caspase activation regardless of which mechanism is employed.

This study determined the ability of QUE and three of its metabolites (RHA, IRHA, and TAM) to exert antioxidant capability, alter A $\beta$  oligomer size distribution, and alter

oligomer conformation. *In vitro* studies revealed that these polyphenols can reduce A $\beta$  oligomer-induced intracellular ROS and caspase activation. However, the difference seen among the polyphenols in attenuating these cellular responses showed that they act through different mechanisms. This study demonstrates that QUE is likely not solely responsible for the attenuation of AD pathology observed in epidemiological studies but that many of the therapeutic effects attributed to QUE are a result of the formation of QUE metabolites which also attenuate oligomer-induced cellular responses.

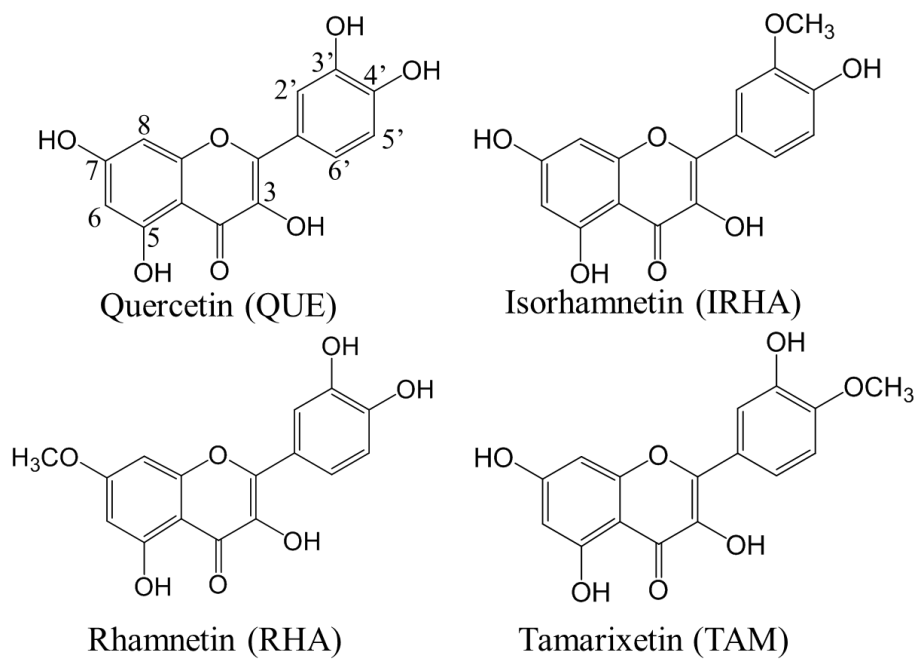


**Figure 4.1 Structure of quercetin metabolites.** Quercetin (QUE) and its metabolites rhamnetin (RHA), isorhamnetin (IRHA), and tamarixetin (TAM).

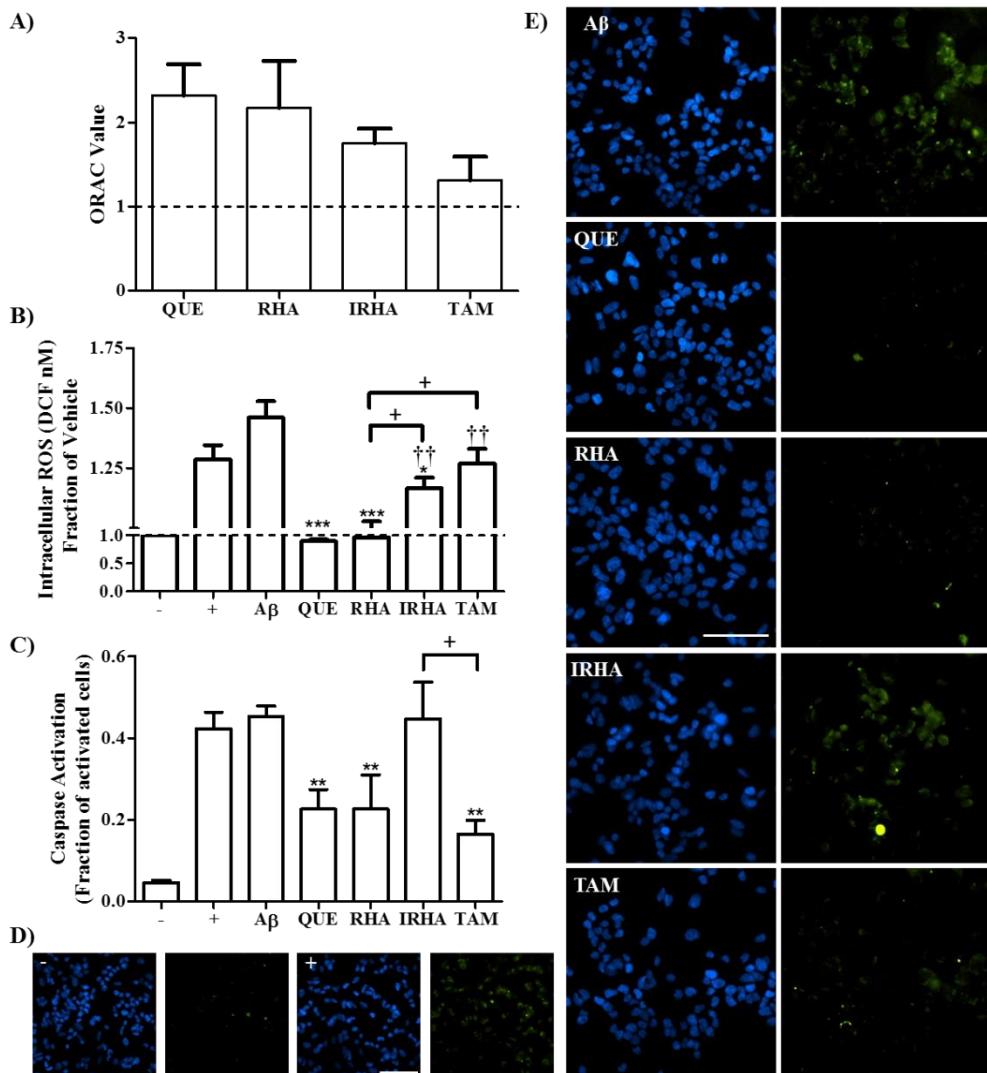


**Figure 4.2 Quercetin and metabolites possess strong antioxidant capability and reduce A $\beta$  oligomer-induced cellular responses.** A) Antioxidant capabilities of quercetin (QUE) and metabolites rhamnetin (RHA), isorhamnetin (IRHA), and tamarixetin (TAM) were assessed using the ORAC assay as described in Section 2.6. Antioxidant capacity is shown as ORAC value which is the equivalent Trolox concentration per molar concentration of polyphenol. ORAC value of Trolox = 1, indicated by the dashed line. Error bars indicate SEM, n=4. SH-SY5Y cells were treated with 0.01  $\mu$ M A $\beta$  oligomers alone (A $\beta$ ) or simultaneously treated with 0.01  $\mu$ M A $\beta$  oligomers and 10  $\mu$ M polyphenol. After 24 h incubation, intracellular ROS and caspase activity was quantified. B) A DCFH-DA probe was used for intracellular ROS quantification. Buffer alone (-) and 25  $\mu$ M H<sub>2</sub>O<sub>2</sub> (+) served as negative and positive controls, respectively. Results are expressed as the intracellular ROS as fraction of negative control. Error bars indicate SEM, C-E) For assessment of caspase activation an Image-iT LIVE Green Poly Caspases detection kit and a Nikon Eclipse 80i fluorescent

microscope was used to acquire nuclear Hoechst (E, left column) and FLICA labeled active caspase (E, right column) images. Buffer alone (-) and 1.5 U/ $\mu$ L TNF- $\alpha$  (+) served as negative and positive controls, respectively (D). Scale bars represent 50  $\mu$ m. Images are representative of 3 independent experiments. Caspase activation was determined using custom MATLAB functions to quantify Hoechst and FLICA images. Results are reported as the fraction (FLICA/Hoechst) of caspase activated cells (C). B-C) Error bars indicate SEM, n=3 for samples, n=12 for controls and A $\beta$  alone. \*p<0.05, \*\*p<0.01, and \*\*\*p<0.001 vs A $\beta$  alone, ††p<0.01 vs QUE and +p<0.05 between samples.

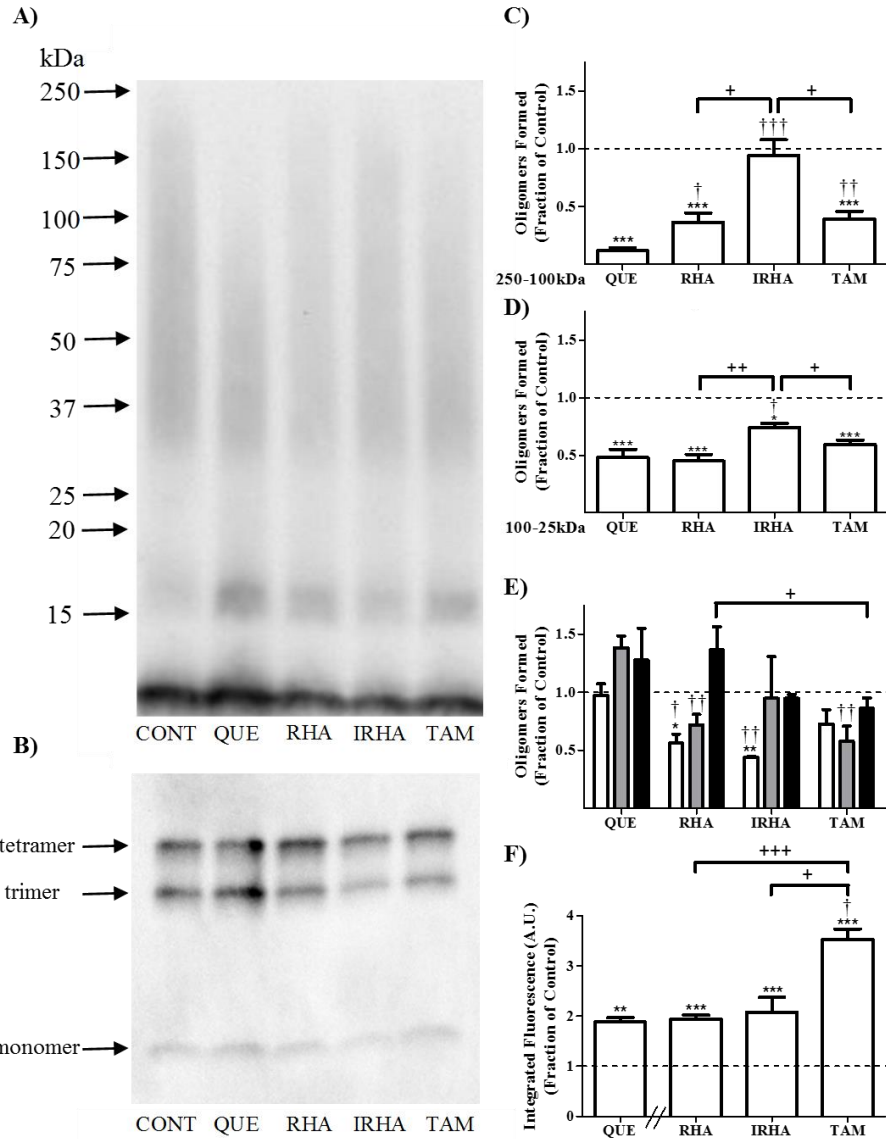


**Figure 4.3 Quercetin and metabolites alter A $\beta$  oligomer size distribution and conformation** A $\beta$  oligomers were prepared as described in Section 2.2. Oligomers were prepared in the absence (control, CONT) or presence of 10-fold excess quercetin (QUE), rhamnetin (RHA), isorhamnetin (IRHA), or tamarixetin (TAM). Final oligomer reactions containing 15  $\mu$ M A $\beta$ , 150  $\mu$ M polyphenol, 1  $\mu$ M NaCl, and 2.5% DMSO were incubated for 30 min (25°C). To determine the amount of oligomers formed, oligomer products were resolved by SDS-PAGE on either A) a 4-20% tris-glycine gel or B) a 16.5% tris-tricine gel, transferred to nitrocellulose membrane, and probed with 6E10 antibody. Images are representative of 3-5 independent experiments. Volumetric analysis was used to quantify oligomer species within size ranges of C) 250-100 kDa and D) 100-25 kDa. E) Band intensity analysis was used to quantify monomer (open bars), trimer (closed bars) and tetramer (grey bars) species. F) To

assess alterations in oligomer conformation, oligomer products were combined with either ANS or Nile Red and the fluorescence emissions were measured as described in Section 2.4 and 2.5. Fluorescence values were determined as the IAUC, corrected by blank subtraction. All results are normalized to the control with a value of 1, indicated by the dashed line, representing no change. Error bars indicate SEM, n=3-5. \* $p<0.05$ , \*\* $p<0.01$ , and \*\*\* $p<0.001$  vs CONT; † $p<0.05$ , ‡ $p<0.01$ , and ‡‡‡ $p<0.001$  vs QUE; + $p<0.05$ , ++ $p<0.01$ , and +++ $p<0.001$  between samples.

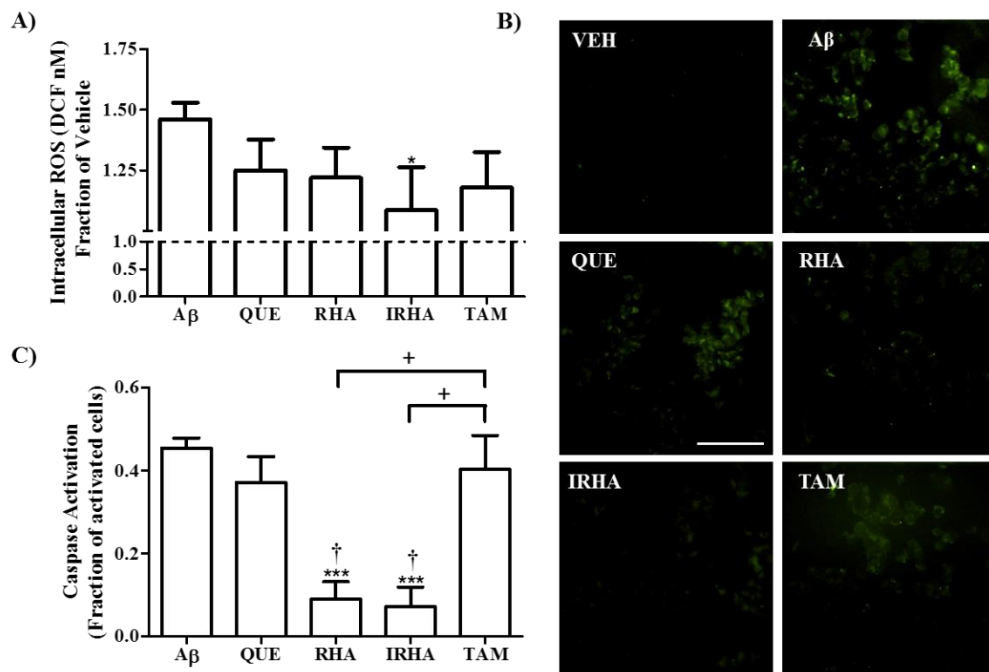


**Figure 4.4 Alterations to A $\beta$  oligomer size distribution and conformation reduce A $\beta$  oligomer-induced cellular responses.** SH-SY5Y cells were treated with 0.01  $\mu$ M A $\beta$  oligomers formed in the absence (A $\beta$ ) or presence of 10-fold excess of polyphenol and incubated for 24 h. A) Intracellular ROS was quantified as described in Figure 4.2. B) FLICA labeled active caspase images were acquired as described in Figure 4.2. Coinciding Hoechst images can be found in Appendix D. Scale bar represents 50 $\mu$ m. Images are representative of 3-4 independent experiments. C) Hoechst and FLICA images were quantified using custom MATLAB functions to determine caspase activation. Results are reported as the fraction (FLICA/Hoechst) of caspase activated cells. A and C) Error bars indicate SEM, n=3-4 for samples, n=12 for A $\beta$  alone. \* p<0.05, and \*\*\* p<0.001 vs A $\beta$  alone; † p<0.05 vs QUE; + p<0.05 between samples.

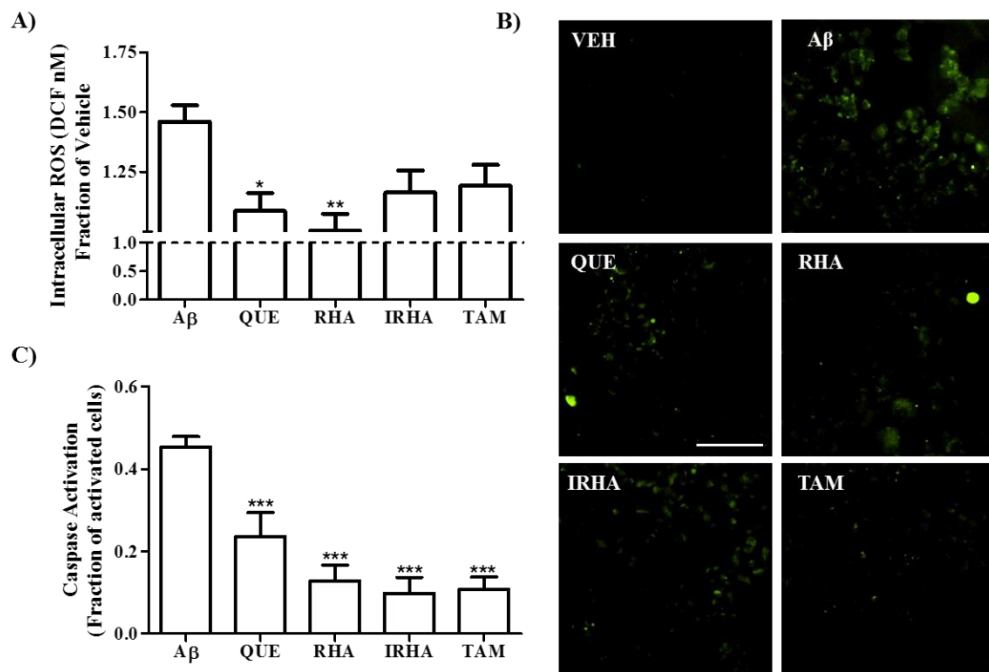


**Figure 4.5 Dual-action potential of quercetin and metabolites to reduce A $\beta$  oligomer-induced cellular responses.** SH-SY5Y cells were treated with 0.01  $\mu$ M A $\beta$  oligomers formed in the absence (A $\beta$ ) or presence of 10-fold excess polyphenols. Cells treated with oligomers formed in the presence of polyphenols were treated simultaneously with an additional 10  $\mu$ M polyphenol as described in Section 4.2.6. Cells were incubated for 24 h. A) Intracellular ROS was quantified as described in Figure 4.2. B) FLICA labeled active caspase images were acquired as described in Figure 4.2. Coinciding Hoechst images can be found in Appendix D. Scale bar represents 50  $\mu$ m. Images are representative of 3-4 independent experiments. C) Hoechst and FLICA images were quantified using custom MATLAB functions to determine caspase activation. Results are reported as the fraction (FLICA/Hoechst) of caspase activated cells. A and C) Error bars indicate SEM, n=3-4 for samples, n=12 for A $\beta$  alone. \* p<0.05, \*\* p<0.01, and \*\*\* p<0.001 vs A $\beta$  alone.

## CHAPTER 5

### CONCLUSIONS

As the number of people with AD continues to rise, so does the desperate need for a therapeutic. Attenuating AD pathology by either targeting A $\beta$  oligomer formation directly or reducing the cellular responses created by oligomers has been one proposed therapeutic strategy. Polyphenols have been suggested as potential natural therapeutics for AD based on epidemiological studies correlating polyphenol-rich diets with a reduced incidence of AD.<sup>47–49,120–123</sup> Based on these and other supporting data, this study sought to identify polyphenols that can reduce A $\beta$  oligomer-induced cellular responses by 1) altering oligomer formation and 2) exerting antioxidant capabilities. The ability of polyphenols to function as dual-action therapeutics for AD by acting through both mechanisms was also explored.

In Chapter 3, several polyphenols were identified that alter oligomer formation by changing the oligomer size distribution. The set of polyphenols examined varied by number and placement of hydroxyl groups, thereby allowing the identification of key structural elements that are crucial for oligomer inhibition. FLA, the only compound with no hydroxyl groups, was unable to alter oligomer size distribution demonstrating the importance of hydroxylation. While the number of hydroxyl groups did not directly correlate with the potential of polyphenols to intervene in oligomer formation, the placement of the hydroxyl groups on the polyphenols did. Addition of a hydroxyl group to the 3 position significantly increased the ability of polyphenols to alter oligomer size

distribution, whereas the presence of a hydroxyl group at the 3' position had a slightly negative impact. In Chapter 4, the effect of substituting a hydroxyl group with a methoxy group was investigated to determine whether hydroxyl groups specifically or just functionalization in general was necessary for effective oligomer inhibition. Results showed that a substitution at the 4' or 7 position had little effect but, that substitution at the 3' position drastically reduced inhibitory capabilities. In Chapter 3, adding a hydroxyl group to the 3' position of KAE (to form QUE) slightly decreased efficacy; however, in Chapter 4 when a methoxy group is added to the same position (to form IRHA) there is nearly a complete loss in all inhibitory capability. This result demonstrates the effect the type of functionalization has on the ability of polyphenols to alter oligomer formation. Together, these findings provide insight into the optimum polyphenol structure to target oligomer formation.

The ability of polyphenols to alter oligomer conformation was also investigated. In Chapter 3, FLA was unable to alter oligomer conformation, again demonstrating the need for polyphenol functionalization. Contrastingly, functionalized polyphenols not only demonstrated the ability to alter oligomer conformation but the ability to do so in opposing ways. LUT significantly reduced oligomer surface hydrophobicity. Conversely, adding a hydroxyl to LUT at the 3 position (to form QUE) yielded the inverse effect: creating oligomers with significantly higher surface hydrophobicity. In Chapter 4, substituting a hydroxyl group with a methoxy group at the 3' or 7 position of QUE did not affect oligomer surface hydrophobicity while substitution at the 4 position significantly increased surface hydrophobicity. These results further demonstrate the importance of the location and type

of functionalization on polyphenols to altering oligomer formation and provide further insight into the optimal polyphenol structure to target oligomerization.

The effect polyphenol-induced changes to oligomer formation had on cellular responses was examined by evaluating changes in intracellular ROS and caspase activation. Alterations to oligomer formation by LUT and IRHA were shown to reduce oligomer-induced intracellular ROS in SH-SY5Y cells. These polyphenols were some of the least effective at shifting oligomer size distribution but still significantly altered oligomer conformation. Therefore, altering oligomer conformation rather than oligomer size distribution could be a key property required for effective AD therapeutics. Additionally, RHA and IRHA attenuated oligomer-induced caspase activation, suggesting that oligomer alterations by polyphenols containing methoxy groups may limit oligomer-cell interactions. Combined, these studies demonstrate that polyphenols have potential as natural therapeutics for AD by altering oligomer formation.

All polyphenols tested exhibited high antioxidant strength; however, a reduction in antioxidant capability was observed for IRHA and TAM which have a disrupted 3', 4'-catechol structure due to a methoxy group substitution. Antioxidant capability was shown to translate into a reduction in A $\beta$  oligomer-induced intracellular ROS with only TAM unable to significantly reduce ROS. Several polyphenols were also able to reduce A $\beta$  oligomer-induced caspase activation via their antioxidant properties. These studies demonstrate that polyphenols have potential as natural therapeutics for AD by reducing oligomer-induced cellular responses via their antioxidant properties.

While the polyphenols in Chapter 3 were observed to predominantly attenuate A $\beta$  oligomer-induced cellular responses through their antioxidant capabilities, some

polyphenols investigated in Chapter 4 were shown to also act through different mechanisms. While QUE and TAM both primarily reduced oligomer-induced cellular responses via their antioxidant properties, IRHA instead attenuated cellular responses by altering oligomer formation. Interestingly, RHA was equally effective at reducing oligomer-induced caspase activation regardless of which mechanism was employed. Unfortunately, simultaneous use of both mechanisms did not significantly improve RHA's impact on cellular responses. KAE, however, did show potential as a dual-action therapeutic with significantly greater reduction of both ROS and caspase when both mechanisms of attenuation were used compared to when either mechanism used alone.

In summary, this study has successfully characterized the ability of several polyphenols to attenuate oligomer-induced cellular responses and identified via which mechanism they accomplish this attenuation. This information will direct future work in identifying the most promising polyphenols for use as natural therapeutics for AD.

## CHAPTER 6

### FUTURE PERSPECTIVES

While only one of the tested polyphenols exhibited dual-action ability, polyphenols were shown to act through different mechanisms to attenuate oligomer-induced cellular responses. Therefore, the potential exists for two polyphenols, acting through different mechanisms, to synergistically attenuate cellular responses. To test this theory, cells would be treated simultaneously with oligomers made in the presence of a polyphenol shown to be effective at reducing cellular responses by altering oligomer formation (RHA or IRHA) and with a polyphenol shown to be effective via their antioxidant capability (LUT, QUE, or TAM). Testing different combinations of the polyphenols indicated above would identify potential therapeutic cocktails that could attenuate AD pathology using two separate mechanisms.

The use of cell culture assays allowed two separate mechanisms by which polyphenols can attenuate oligomer-induced cellular responses to be explored. However, these observed effects may not translate into effective oral therapeutics considering the extent to which many polyphenols are metabolized *in vivo* and the need for the polyphenols to cross the blood-brain barrier. Therefore, animal models are needed to further characterize the potential of promising polyphenols as natural therapeutics for AD. Several mouse models of AD have been designed, such as the Tg-SwDi mouse model that develops neuronal and vascular amyloid pathology as well as brain-associated inflammation.<sup>166,167</sup> Daily administration of polyphenols to these mice for several months prior to the onset of

A $\beta$  deposition and memory deficits would determine the impact of long-term exposure to polyphenols on AD pathology. The effects of polyphenol administration could be assessed by using behavior testing, such as the Morris water maze test and contextual fear conditioning, and by evaluating AD pathology markers such as A $\beta$  burden and cerebral inflammation.<sup>168</sup> Combined, these additional studies would further determine which polyphenols are best suited for use as natural therapeutics for AD and thus direct future drug development.

## REFERENCES

1. Alzheimer's Association. 2015 Alzheimer's disease facts and figures. *Alzheimers. Dement.* **11**, 332–84 (2015).
2. Alzheimer's Association. Alzheimer's disease facts and figures. *Alzheimer's Dement.* **9**, 110 –133. (2013).
3. National Institute of Aging. Alzheimer's Disease Medications. *NIH Publ. No. 15-3431* (2015).
4. Chen, Q. S., Kagan, B. L., Hirakura, Y. & Xie, C. W. Impairment of hippocampal long-term potentiation by Alzheimer amyloid  $\beta$ -peptides. *J. Neurosci. Res.* **60**, 65–72 (2000).
5. McKhann, G. *et al.* Clinical diagnosis of Alzheimer's disease: report of the NINCDS-ADRDA Work Group under the auspices of Department of Health and Human Services Task Force on Alzheimer's Disease. *Neurology* **34**, 939–944 (1984).
6. Cleary, J. P. *et al.* Natural oligomers of the amyloid- $\beta$  protein specifically disrupt cognitive function. *Nat. Neurosci.* **8**, 79–84 (2005).
7. Alzheimer, A. Über eine eigenartige Erkrankung der Hirnrinde. *Allg Zeits Psychiatrie Psych. Med* **64**, 146–8 (1907).
8. Goedert, M. & Spillantini, M. G. A century of Alzheimer's disease. *Science* **314**, 777–81 (2006).
9. Ittner, L. M. & Götz, J. Amyloid- $\beta$  and tau--a toxic pas de deux in Alzheimer's disease. *Nat. Rev. Neurosci.* **12**, 65–72 (2011).
10. Oddo, S., Billings, L., Kesslak, J. P., Cribbs, D. H. & LaFerla, F. M. A $\beta$  immunotherapy leads to clearance of early, but not late, hyperphosphorylated tau aggregates via the proteasome. *Neuron* **43**, 321–332 (2004).
11. Oddo, S., Caccamo, A., Kitazawa, M., Tseng, B. P. & LaFerla, F. M. Amyloid deposition precedes tangle formation in a triple transgenic model of Alzheimer's disease. in *Neurobiol. Aging* **24**, 1063–1070 (2003).
12. Hardy, J. & Selkoe, D. J. The amyloid hypothesis of Alzheimer's disease: progress and problems on the road to therapeutics. *Science* **297**, 353–356 (2002).
13. Lewis, J. *et al.* Enhanced Neurofibrillary Degeneration in Transgenic Mice Expressing Mutant Tau and APP. *J. Chem. Inf. Model.* **293**, 1487–1491 (2001).

14. Bayer, T. a, Cappai, R., Masters, C. L., Beyreuther, K. & Multhaup, G. It all sticks together--the APP-related family of proteins and Alzheimer's disease. *Mol. Psychiatry* **4**, 524–528 (1999).
15. Kang, J. *et al.* The precursor of Alzheimer's disease amyloid A4 protein resembles a cell-surface receptor. *Nature* **325**, 733–736 (1987).
16. Selkoe, D. Alzheimer's Disease: A Central Role for Amyloid. *J. Neuropathol. Exp. Neurol.* **53**, 438–447 (1994).
17. Roher, a E. *et al.*  $\beta$ -Amyloid-(1-42) is a Major Component of Cerebrovascular Amyloid Deposits: Implications for the Pathology of Alzheimer Disease. *Proc. Natl. Acad. Sci.* **90**, 10836–10840 (1993).
18. Selkoe, D. J. & Schenk, D. Alzheimer's disease: molecular understanding predicts amyloid-based therapeutics. *Annu. Rev. Pharmacol. Toxicol.* **43**, 545–584 (2003).
19. Mehta, P. D. *et al.* Plasma and cerebrospinal fluid levels of amyloid  $\beta$  proteins 1-40 and 1-42 in Alzheimer disease. *Arch. Neurol.* **57**, 100–105 (2000).
20. Klein, W. L., Krafft, G. A. & Finch, C. E. Targeting small A $\beta$  oligomers: The solution to an Alzheimer's disease conundrum? *Trends Neurosci.* **24**, 219–224 (2001).
21. Mucke, L. *et al.* High-level neuronal expression of A $\beta_{1-42}$  in wild-type human amyloid protein precursor transgenic mice: synaptotoxicity without plaque formation. *J. Neurosci.* **20**, 4050–4058 (2000).
22. Hsai, A. Y. *et al.* Plaque-independent disruption of neural circuits in Alzheimer's disease mouse models. *Proc. Natl. Acad. Sci. U. S. A.* **96**, 3228–33 (1999).
23. Benilova, I., Karran, E. & De Strooper, B. The toxic A $\beta$  oligomer and Alzheimer's disease: an emperor in need of clothes. *Nat. Neurosci.* **15**, 349–57 (2012).
24. McLean, C. A. *et al.* Soluble pool of A $\beta$  amyloid as a determinant of severity of neurodegeneration in Alzheimer's disease. *Ann. Neurol.* **46**, 860–866 (1999).
25. Mc Donald, J. M. *et al.* The presence of sodium dodecyl sulphate-stable A $\beta$  dimers is strongly associated with Alzheimer-type dementia. *Brain* **133**, 1328–41 (2010).
26. Lambert, M. P. *et al.* Diffusible, nonfibrillar ligands derived from A $\beta_{1-42}$  are potent central nervous system neurotoxins. *Proc. Natl. Acad. Sci. U. S. A.* **95**, 6448–53 (1998).
27. Shankar, G. M. *et al.* Natural Oligomers of the Alzheimer Amyloid- $\beta$  Protein Induce Reversible Synapse Loss by Modulating an NMDA-Type Glutamate Receptor-Dependent Signaling Pathway. *J. Neurosci.* **27**, 2866–2875 (2007).
28. Walsh, D. M. & Selkoe, D. J. A $\beta$  oligomers - A decade of discovery. *J. Neurochem.* **101**, 1172–1184 (2007).
29. Kirkpatrick, M. D., Bitan, G. & Teplow, D. B. Paradigm shifts in Alzheimer's disease and other neuro degenerative disorders: The emerging role of oligomeric assemblies. *J. Neurosci. Res.* **69**, 567–577 (2002).

30. Lesné, S. *et al.* A specific amyloid- $\beta$  protein assembly in the brain impairs memory. *Nature* **440**, 352–357 (2006).
31. Gonzalez-Velasquez, F. J., Kotarek, J. A. & Moss, M. A. Soluble aggregates of the amyloid- $\beta$  protein selectively stimulate permeability in human brain microvascular endothelial monolayers. *J. Neurochem.* **107**, 466–77 (2008).
32. Gonzalez-Velasquez, F. J. & Moss, M. A. Soluble aggregates of the amyloid- $\beta$  protein activate endothelial monolayers for adhesion and subsequent transmigration of monocyte cells. *J. Neurochem.* **104**, 500–513 (2008).
33. Zhao, B. Natural antioxidants for neurodegenerative diseases. *Mol. Neurobiol.* **31**, 283–293 (2005).
34. Viña, J. *et al.* Mitochondrial oxidant signalling in Alzheimer's disease. *J. Alzheimers. Dis.* **11**, 175–81 (2007).
35. Smith, W. W., Gorospe, M. & Kusiak, J. W. Signaling mechanisms underlying A $\beta$  toxicity: potential therapeutic targets for Alzheimer's disease. *CNS Neurol Disord Drug Targets* **5**, 355–361 (2006).
36. Block, M. L. NADPH oxidase as a therapeutic target in Alzheimer's disease. *BMC Neurosci.* **9 Suppl 2**, S8 (2008).
37. Eckert, A. *et al.* Mitochondrial dysfunction, apoptotic cell death, and Alzheimer's disease. in *Biochem. Pharmacol.* **66**, 1627–1634 (2003).
38. McIlwain, D. R., Berger, T. & Mak, T. W. Caspase functions in cell death and disease. *Cold Spring Harb. Perspect. Biol.* **5**, 1–28 (2013).
39. Salminen, A., Ojala, J., Kauppinen, A., Kaarniranta, K. & Suuronen, T. Inflammation in Alzheimer's disease: Amyloid- $\beta$  oligomers trigger innate immunity defence via pattern recognition receptors. *Prog. Neurobiol.* **87**, 181–194 (2009).
40. Viola, K. L. & Klein, W. L. Amyloid  $\beta$  oligomers in Alzheimer's disease pathogenesis, treatment, and diagnosis. *Acta Neuropathol.* **129**, 183–206 (2015).
41. Ladiwala, A. R. A. *et al.* Conformational differences between two amyloid  $\beta$  oligomers of similar size and dissimilar toxicity. *J. Biol. Chem.* **287**, 24765–24773 (2012).
42. Breydo, L. & Uversky, V. N. Structural, morphological, and functional diversity of amyloid oligomers. *FEBS Lett.* **589**, 2640–2648 (2015).
43. Galante, D. *et al.* Differential toxicity, conformation and morphology of typical initial aggregation states of A $\beta$ 1-42 and A $\beta$ y3-42 beta-amyloids. *Int. J. Biochem. Cell Biol.* **44**, 2085–2093 (2012).
44. Porat, Y., Abramowitz, A. & Gazit, E. Inhibition of amyloid fibril formation by polyphenols: Structural similarity and aromatic interactions as a common inhibition mechanism. *Chem. Biol. Drug Des.* **67**, 27–37 (2006).
45. Lorenzo, A. & Yankner, B. A.  $\beta$ -amyloid neurotoxicity requires fibril formation and is inhibited by congo red. *Proc. Natl. Acad. Sci. U. S. A.* **91**, 12243–12247 (1994).

46. Lee, V. M. Y. Amyloid binding ligands as Alzheimer's disease therapies. *Neurobiol. Aging* **23**, 1039–1042 (2002).
47. Butterfield, D. A. *et al.* Nutritional approaches to combat oxidative stress in Alzheimer's disease. *J. Nutr. Biochem.* **13**, 444–461 (2002).
48. Dai, Q., Borenstein, A. R., Wu, Y., Jackson, J. C. & Larson, E. B. Fruit and Vegetable Juices and Alzheimer's Disease: The Kame Project. *Am. J. Med.* **119**, 751–759 (2006).
49. Barberger-Gateau, P. *et al.* Dietary patterns and risk of dementia: The Three-City cohort study. *Neurology* **69**, 1921–1930 (2007).
50. Lemkul, J. A. & Bevan, D. R. Destabilizing Alzheimer's A $\beta$ <sub>42</sub> Protofibrils with Morin: Mechanistic Insights from Molecular Dynamics Simulations. *Biochemistry* **49**, 3935–3946 (2010).
51. Williams, R. J. & Spencer, J. P. E. Flavonoids, cognition, and dementia: Actions, mechanisms, and potential therapeutic utility for Alzheimer disease. *Free Radic. Biol. Med.* **52**, 35–45 (2012).
52. Ono, K. *et al.* Potent anti-amyloidogenic and fibril-destabilizing effects of polyphenols in vitro: Implications for the prevention and therapeutics of Alzheimer's disease. *J. Neurochem.* **87**, 172–181 (2003).
53. Rivière, C. *et al.* New polyphenols active on  $\beta$ -amyloid aggregation. *Bioorganic Med. Chem. Lett.* **18**, 828–831 (2008).
54. Yang, F. *et al.* Curcumin inhibits formation of amyloid  $\beta$  oligomers and fibrils, binds plaques, and reduces amyloid in vivo. *J. Biol. Chem.* **280**, 5892–5901 (2005).
55. Rivière, C. *et al.* Inhibitory activity of stilbenes on Alzheimer's  $\beta$ -amyloid fibrils in vitro. *Bioorganic Med. Chem.* **15**, 1160–1167 (2007).
56. Bandyopadhyay, P., Ghosh, A. K. & Ghosh, C. Recent developments on polyphenol–protein interactions: effects on tea and coffee taste, antioxidant properties and the digestive system. *Food Funct.* **3**, 592–605 (2012).
57. Ono, K. *et al.* Effects of grape seed-derived polyphenols on amyloid  $\beta$ -protein self-assembly and cytotoxicity. *J. Biol. Chem.* **283**, 32176–32187 (2008).
58. Pitt, J. *et al.* Alzheimer's-associated A $\beta$  oligomers show altered structure, immunoreactivity and synaptotoxicity with low doses of oleocanthal. *Toxicol. Appl. Pharmacol.* **240**, 189–197 (2009).
59. Feng, Z. & Zhang, J. T. Melatonin reduces amyloid  $\beta$ -induced apoptosis in pheochromocytoma (PC12) cells. *J. Pineal Res.* **37**, 257–266 (2004).
60. Xiao, X. Q., Zhang, H. Y. & Tang, X. C. Huperzine A attenuates amyloid  $\beta$ -peptide fragment 25–35-induced apoptosis in rat cortical neurons via inhibiting reactive oxygen species formation and caspase-3 activation. *J. Neurosci. Res.* **67**, 30–6 (2002).

61. Singh, M., Arseneault, M., Sanderson, T., Murthy, V. & Ramassamy, C. Challenges for research on polyphenols from foods in Alzheimer's disease: Bioavailability, metabolism, and cellular and molecular mechanisms. *J. Agric. Food Chem.* **56**, 4855–4873 (2008).
62. Kelley, B. J. & Knopman, D. S. Alternative medicine and Alzheimer disease. *Neurologist* **14**, 299–306 (2008).
63. Sun, A. Y., Wang, Q., Simonyi, A. & Sun, G. Y. Botanical phenolics and brain health. *NeuroMolecular Med.* **10**, 259–274 (2008).
64. Darvesh, A. S., Carroll, R. T., Bishayee, A., Geldenhuys, W. J. & Van der Schyf, C. J. Oxidative stress and Alzheimer's disease: dietary polyphenols as potential therapeutic agents. *Expert Rev. Neurother.* **10**, 729–745 (2010).
65. Li, J., O, W., Li, W., Jiang, Z.-G. & Ghanbari, H. A. Oxidative stress and neurodegenerative disorders. *Int. J. Mol. Sci.* **14**, 24438–75 (2013).
66. Ansari, M. A., Abdul, H. M., Joshi, G., Opie, W. O. & Butterfield, D. A. Protective effect of quercetin in primary neurons against A $\beta$ (1-42): relevance to Alzheimer's disease. *J. Nutr. Biochem.* **20**, 269–75 (2009).
67. Oliveira, G. L. da S., Oliveira, F. R. de A. M. de & Freitas, R. M. de. Potential involvement of oxidative stress in induction of neurodegenerative diseases: Actions, mechanisms and neurotherapeutic potential of natural antioxidants. *African J. Pharm. Pharmacol.* **8**, 685–700 (2014).
68. Li, Y. *et al.* Quercetin protects human brain microvascular endothelial cells from fibrillar  $\beta$ -amyloid<sub>1-40</sub>-induced toxicity. *Acta Pharm. Sin. B* **5**, 47–54 (2015).
69. Stefani, M. & Rigacci, S. Protein folding and aggregation into amyloid: the interference by natural phenolic compounds. *Int. J. Mol. Sci.* **14**, 12411–12457 (2013).
70. Kim, H. *et al.* Effects of naturally occurring compounds on fibril formation and oxidative stress of  $\beta$ -amyloid. *J. Agric. Food Chem.* **53**, 8537–8541 (2005).
71. Prior, R. L. & Cao, G. Antioxidant Capacity and Polyphenols Components of Teas: Implications for Altering In Vivo Antioxidant Status. *Exp. Biol. Med.* **220**, 255–261 (1999).
72. Miller, K. B. *et al.* Antioxidant Activity and Polyphenol and Procyanoanidin Contents of Selected Commercially Available Cocoa-Containing and Chocolate Products in the United States. *J. Agric. Food Chem.* **54**, 4062–4068 (2006).
73. Silva, E. M., Souza, J. N. S., Rogez, H., Rees, J. F. & Larondelle, Y. Antioxidant activities and polyphenolic contents of fifteen selected plant species from the Amazonian region. *Food Chem.* **101**, 1012–1018 (2006).
74. Lindgren, M. & Hammarström, P. Amyloid oligomers: Spectroscopic characterization of amyloidogenic protein states. *FEBS J.* **277**, 1380–1388 (2010).

75. Fändrich, M. Oligomeric intermediates in amyloid formation: Structure determination and mechanisms of toxicity. *J. Mol. Biol.* **421**, 427–440 (2012).
76. Bolognesi, B. *et al.* ANS binding reveals common features of cytotoxic amyloid species. *ACS Chem. Biol.* **5**, 735–740 (2010).
77. Hawe, A., Sutter, M. & Jiskoot, W. Extrinsic fluorescent dyes as tools for protein characterization. *Pharm. Res.* **25**, 1487–1499 (2008).
78. Yanagi, K. *et al.* Hexafluoroisopropanol induces amyloid fibrils of islet amyloid polypeptide by enhancing both hydrophobic and electrostatic interactions. *J. Biol. Chem.* **286**, 23959–23966 (2011).
79. Williams, R. J. & Spencer, J. P. E. Flavonoids, cognition, and dementia: Actions, mechanisms, and potential therapeutic utility for Alzheimer disease. *Free Radic. Biol. Med.* **52**, 35–45 (2012).
80. Ono, K. *et al.* Potent anti-amyloidogenic and fibril-destabilizing effects of polyphenols in vitro: Implications for the prevention and therapeutics of Alzheimer's disease. *J. Neurochem.* **87**, 172–181 (2003).
81. Zuo, L. & Motherwell, M. S. The impact of reactive oxygen species and genetic mitochondrial mutations in Parkinson's disease. *Gene* **532**, 18–23 (2013).
82. Zuo, L., Hemmelgarn, B. T., Chuang, C.-C. & Best, T. M. The Role of Oxidative Stress-Induced Epigenetic Alterations in Amyloid- $\beta$  Production in Alzheimer's Disease. *Oxid. Med. Cell. Longev.* **2015**, (2014).
83. Porat, Y., Abramowitz, A. & Gazit, E. Inhibition of amyloid fibril formation by polyphenols: Structural similarity and aromatic interactions as a common inhibition mechanism. *Chem. Biol. Drug Des.* **67**, 27–37 (2006).
84. Di Carlo, G., Mascolo, N., Izzo, A. A. & Capasso, F. Flavovoids: old and new aspects of a class of natural therapeutic drugs. *Life Sci.* **65**, 337–353 (1999).
85. Angelo, A. I. PAF and the Digestive Tract. A Review. *J. Pharm. Pharmacol.* **48**, 1103–1111 (1996).
86. Beil, W., Birkholz, C. & Sewing, K. F. Effects of flavonoids on parietal cell acid secretion, gastric mucosal prostaglandin production and Helicobacter pylori growth. *Arzneimittelforschung*. **45**, 697–700 (1995).
87. Landolfi, R., Mower, R. L. & Steiner, M. Modification of platelet function and arachidonic acid metabolism by bioflavonoids. Structure-activity relations. *Biochem. Pharmacol.* **33**, 1525–1530 (1984).
88. Larocca, L. M. *et al.* Growth-inhibitory effect of quercetin and presence of type II estrogen binding sites in primary human transitional cell carcinomas. *J. Urol.* **152**, 1029–1033 (1994).
89. Avila, M. A., Velasco, J. A., Cansado, J. & Notario, V. Quercetin mediates the Down-regulation of mutant p53 in the human breast cancer cell line MDA-MB468. *Cancer Res.* **54**, 2424–2428 (1994).

90. Bitan, G. *et al.* Amyloid  $\beta$ -protein (A $\beta$ ) assembly: A $\beta$ 40 and A $\beta$ 42 oligomerize through distinct pathways. *Proc. Natl. Acad. Sci. U. S. A.* **100**, 330–335 (2003).
91. Gough, D. R. & Cotter, T. G. Hydrogen peroxide: a Jekyll and Hyde signalling molecule. *Cell Death Dis.* **2**, e213 (2011).
92. Veal, E. A., Day, A. M. & Morgan, B. A. Hydrogen peroxide sensing and signaling. *Mol. Cell* **26**, 1–14 (2007).
93. Giorgio, M., Trinei, M., Migliaccio, E. & Pelicci, P. G. Hydrogen peroxide: a metabolic by-product or a common mediator of ageing signals? *Nat. Rev. Mol. Cell Biol.* **8**, 722–8 (2007).
94. Tanabe, A., Shiraishi, M. & Sasaki, Y. Myristoylated Alanine-Rich C Kinase Substrate Accelerates TNF- $\alpha$ -Induced Apoptosis in SH-SY5Y Cells in a Caspases-6 and/or -7-Dependent Manner. *Adv. Biosci. Biotechnol.* **06**, 572–582 (2015).
95. Pregi, N., Wenker, S., Vittori, D., Leirós, C. P. & Nesse, A. TNF-alpha-induced apoptosis is prevented by erythropoietin treatment on SH-SY5Y cells. *Exp. Cell Res.* **315**, 419–31 (2009).
96. Prajapati, P. *et al.* TNF- $\alpha$  regulates miRNA targeting mitochondrial complex-I and induces cell death in dopaminergic cells. *Biochim. Biophys. Acta* **1852**, 451–61 (2015).
97. Sponne, I. *et al.* Membrane cholesterol interferes with neuronal apoptosis induced by soluble oligomers but not fibrils of amyloid- $\beta$  peptide. *FASEB J.* **18**, 836–838 (2004).
98. Deshpande, A., Mina, E., Glabe, C. & Busciglio, J. Different conformations of amyloid  $\beta$  induce neurotoxicity by distinct mechanisms in human cortical neurons. *J. Neurosci. Off. J. Soc. Neurosci.* **26**, 6011–6018 (2006).
99. Malaplate-Armand, C. *et al.* Soluble oligomers of amyloid- $\beta$  peptide induce neuronal apoptosis by activating a cPLA<sub>2</sub>-dependent sphingomyelinase-ceramide pathway. *Neurobiol. Dis.* **23**, 178–189 (2006).
100. Shelat, P. B. *et al.* Amyloid beta peptide and NMDA induce ROS from NADPH oxidase and AA release from cytosolic phospholipase A<sub>2</sub> in cortical neurons. *J. Neurochem.* **106**, 45–55 (2008).
101. He, Y. *et al.* Prolonged exposure of cortical neurons to oligomeric amyloid- $\beta$  impairs NMDA receptor function via NADPH oxidase-mediated ROS production: protective effect of green tea (-)-epigallocatechin-3-gallate. *ASN Neuro* **3**, e00050 (2011).
102. Salminen, A., Ojala, J., Kauppinen, A., Kaarniranta, K. & Suuronen, T. Inflammation in Alzheimer's disease: Amyloid- $\beta$  oligomers trigger innate immunity defence via pattern recognition receptors. *Prog. Neurobiol.* **87**, 181–194 (2009).
103. Yordi, E. G., Pérez, E. M., Matos, M. J. & Villares, E. U. Antioxidant and Pro-Oxidant Effects of Polyphenolic Compounds and Structure-Activity Relationship Evidence. *Nutr. Well-Being Heal.* 23–48 (2012). doi:10.5772/1864

104. Cheung, A. W. H. *et al.* Flavonoids possess neuroprotective effects on cultured pheochromocytoma PC12 cells: A comparison of different flavonoids in activating estrogenic effect and in preventing  $\beta$ -amyloid-induced cell death. *J. Agric. Food Chem.* **55**, 2438–2445 (2007).
105. Cao, G., Sofic, E. & Prior, R. L. Antioxidant and Prooxidant Behavior of Flavonoids: Structure-Activity Relationships. *Free Radic. Biol. Med.* **22**, 749–760 (2348).
106. Scalbert, A., Johnson, I. T. & Saltmarsh, M. Polyphenols: antioxidants and beyond. *Am. J. Clin. Nutr.* **81**, 215–217 (2005).
107. Ishige, K., Schubert, D. & Sagara, Y. Flavonoids protect neuronal cells from oxidative stress by three distinct mechanisms. *Free Radic. Biol. Med.* **30**, 433–446 (2001).
108. Bastianetto, S. & Quirion, R. Natural extracts as possible protective agents of brain aging. *Neurobiol. Aging* **23**, 891–897 (2002).
109. Ladiwala, A. R. a *et al.* Conformational differences between two amyloid  $\beta$  oligomers of similar size and dissimilar toxicity. *J. Biol. Chem.* **287**, 24765–73 (2012).
110. Viola, K. L. & Klein, W. L. Amyloid  $\beta$  oligomers in Alzheimer's disease pathogenesis, treatment, and diagnosis. *Acta Neuropathol.* **129**, 183–206 (2015).
111. Jang, H. *et al.* Alzheimer's disease: which type of amyloid-preventing drug agents to employ? *Phys. Chem. Chem. Phys.* **15**, 8868–77 (2013).
112. Sharoar, M. G. *et al.* Keampferol-3-O-rhamnoside abrogates amyloid beta toxicity by modulating monomers and remodeling oligomers and fibrils to non-toxic aggregates. *J. Biomed. Sci.* **19**, 104 (2012).
113. Ushikubo, H. *et al.* 3,3',4',5,5'-Pentahydroxyflavone is a potent inhibitor of amyloid  $\beta$  fibril formation. *Neurosci. Lett.* **513**, 51–56 (2012).
114. Akaishi, T. *et al.* Structural requirements for the flavonoid fisetin in inhibiting fibril formation of amyloid  $\beta$  protein. *Neurosci. Lett.* **444**, 280–285 (2008).
115. DaSilva, K. A., Shaw, J. E. & McLaurin, J. Amyloid- $\beta$  fibrillogenesis: Structural insight and therapeutic intervention. *Exp. Neurol.* **223**, 311–321 (2010).
116. Kovacic, P., Somanathan, R. & Z. Abadjian, M.-C. Natural Monophenols as Therapeutics, Antioxidants and Toxins; Electron Transfer, Radicals and Oxidative Stress. *Nat. Prod. Journal*, **5**, 142–151 (2015).
117. Chang, S. K., Alasalvar, C. & Shahidi, F. Review of dried fruits: Phytochemicals, antioxidant efficacies, and health benefits. *J. Funct. Foods* **21**, 113–132 (2016).
118. Day, B. J. Antioxidants as potential therapeutics for lung fibrosis. *Antioxid. Redox Signal.* **10**, 355–70 (2008).
119. Halliwell, B., Gutteridge, J. M. C. & Cross, C. E. Free radicals, antioxidants, and human disease: Where are we now? *Transl. Res.* **119**, 598–620 (1992).

120. Buckland, G. & Gonzalez, C. A. The role of olive oil in disease prevention: a focus on the recent epidemiological evidence from cohort studies and dietary intervention trials. *Br. J. Nutr.* **113**, S94–S101 (2015).
121. Scalbert, A., Manach, C., Morand, C., Rémésy, C. & Jiménez, L. Dietary polyphenols and the prevention of diseases. *Crit. Rev. Food Sci. Nutr.* **45**, 287–306 (2005).
122. Liu, J., Xing, J. & Fei, Y. Green tea (*Camellia sinensis*) and cancer prevention: a systematic review of randomized trials and epidemiological studies. *Chin. Med.* **3**, 12 (2008).
123. Le Marchand, L. Cancer preventive effects of flavonoids—a review. *Biomed. Pharmacother.* **56**, 296–301 (2002).
124. Erlund, I. Review of the flavonoids quercetin, hesperetin, and naringenin. Dietary sources, bioactivities, bioavailability, and epidemiology. *Nutr. Res.* **24**, 851–874 (2004).
125. Hertog, M. G., Hollman, P. C., Katan, M. B. & Kromhout, D. Intake of potentially anticarcinogenic flavonoids and their determinants in adults in The Netherlands. *Nutr. Cancer* **20**, 21–9 (1993).
126. Perez-Vizcaino, F. Endothelium-Independent Vasodilator Effects of the Flavonoid Quercetin and Its Methylated Metabolites in Rat Conductance and Resistance Arteries. *J. Pharmacol. Exp. Ther.* **302**, 66–72 (2002).
127. Scalbert, A. & Williamson, G. Dietary Intake and Bioavailability of Polyphenols. *J. Nutr.* **130**, 2073S–2085 (2000).
128. Spencer, J. P. E., Abd El Mohsen, M. M. & Rice-Evans, C. Cellular uptake and metabolism of flavonoids and their metabolites: implications for their bioactivity. *Arch. Biochem. Biophys.* **423**, 148–161 (2004).
129. Spencer, J. P. E., Kuhnle, G. G. C., Williams, R. J. & Rice-Evans, C. Intracellular metabolism and bioactivity of quercetin and its in vivo metabolites. *Biochem. J.* **372**, 173–81 (2003).
130. Manach, C., Williamson, G., Morand, C., Scalbert, A. & Rémésy, C. Bioavailability and bioefficacy of polyphenols in humans. I. Review of 97 bioavailability studies. *Am. J. Clin. Nutr.* **81**, (2005).
131. Boesch-Saadatmandi, C. *et al.* Effect of quercetin and its metabolites isorhamnetin and quercetin-3-glucuronide on inflammatory gene expression: Role of miR-155. *J. Nutr. Biochem.* **22**, 293–299 (2011).
132. Ebrahimi, A. & Schlueter, H. Natural polyphenols against neurodegenerative disorders: Potentials and pitfalls. *Ageing Res. Rev.* **11**, 329–345 (2012).
133. Christen, Y. Oxidative stress and Alzheimer disease. *Am. J. Clin. Nutr.* **71**, 621S–629S (2000).

134. Varadarajan, S., Yatin, S., Aksenova, M. & Butterfield, D. A. Review: Alzheimer's amyloid  $\beta$ -peptide-associated free radical oxidative stress and neurotoxicity. *J. Struct. Biol.* **130**, 184–208 (2000).
135. Murakami, K. *et al.* SOD<sub>1</sub> (copper/zinc superoxide dismutase) deficiency drives amyloid  $\beta$  protein oligomerization and memory loss in mouse model of Alzheimer disease. *J. Biol. Chem.* **286**, 44557–44568 (2011).
136. Chandra, J., Samali, A. & Orrenius, S. Triggering and modulation of apoptosis by oxidative stress. *Free Radic. Biol. Med.* **29**, 323–333 (2000).
137. Annunziato, L. *et al.* Apoptosis induced in neuronal cells by oxidative stress: role played by caspases and intracellular calcium ions. *Toxicol. Lett.* **139**, 125–133 (2003).
138. Kannan, K. & Jain, S. K. Oxidative stress and apoptosis. *Pathophysiology* **7**, 153–163 (2000).
139. Junn, E. & Mouradian, M. M. Apoptotic signaling in dopamine-induced cell death: the role of oxidative stress, p38 mitogen-activated protein kinase, cytochrome c and caspases. *J. Neurochem.* **78**, 374–383 (2001).
140. Lagoa, R., Graziani, I., Lopez-Sanchez, C., Garcia-Martinez, V. & Gutierrez-Merino, C. Complex I and cytochrome c are molecular targets of flavonoids that inhibit hydrogen peroxide production by mitochondria. *Biochim. Biophys. Acta - Bioenerg.* **1807**, 1562–1572 (2011).
141. Kim, Y. J. Rhamnetin attenuates melanogenesis by suppressing oxidative stress and pro-inflammatory mediators. *Biol. Pharm. Bull.* **36**, 1341–7 (2013).
142. Park, E. S. *et al.* Cardioprotective effects of rhamnetin in H9c2 cardiomyoblast cells under H<sub>2</sub>O<sub>2</sub>-induced apoptosis. *J. Ethnopharmacol.* **153**, 552–560 (2014).
143. Shi, C. *et al.* Protective effects of Ginkgo biloba extract (EGb761) and its constituents quercetin and ginkgolide B against  $\beta$ -amyloid peptide-induced toxicity in SH-SY5Y cells. *Chem. Biol. Interact.* **181**, 115–123 (2009).
144. Heim, K. E., Tagliaferro, A. R. & Bobilya, D. J. Flavonoid antioxidants: Chemistry, metabolism and structure-activity relationships. *J. Nutr. Biochem.* **13**, 572–584 (2002).
145. Dugas, A. J. *et al.* Evaluation of the total peroxyxyl radical-scavenging capacity of flavonoids: Structure-activity relationships. *J. Nat. Prod.* **63**, 327–331 (2000).
146. Sekher Pannala, A., Chan, T. S., O'Brien, P. J. & Rice-Evans, C. A. Flavonoid B-ring chemistry and antioxidant activity: fast reaction kinetics. *Biochem. Biophys. Res. Commun.* **282**, 1161–1168 (2001).
147. Sun, B. *et al.* Isorhamnetin inhibits H<sub>2</sub>O<sub>2</sub>-induced activation of the intrinsic apoptotic pathway in H9c2 cardiomyocytes through scavenging reactive oxygen species and ERK inactivation. *J. Cell. Biochem.* **113**, 473–485 (2012).

148. Rusak, G., Gutzeit, H. O. & Müller, J. L. Structurally related flavonoids with antioxidative properties differentially affect cell cycle progression and apoptosis of human acute leukemia cells. *Nutr. Res.* **25**, 143–155 (2005).
149. Mohan, M. *et al.* Antioxidants prevent UV-induced apoptosis by inhibiting mitochondrial cytochrome c release and caspase activation in *Spodoptera frugiperda* (Sf9) cells. *Cell Biol. Int.* **27**, 483–490 (2003).
150. Williams, R. J., Spencer, J. P. E. & Rice-Evans, C. Flavonoids: antioxidants or signalling molecules? *Free Radic. Biol. Med.* **36**, 838–49 (2004).
151. Echeverry, C. *et al.* Pretreatment with natural flavones and neuronal cell survival after oxidative stress: A structure-activity relationship study. *J. Agric. Food Chem.* **58**, 2111–2115 (2010).
152. Min, B. S. *et al.* Cholinesterase inhibitors from *Cleistocalyx operculatus* buds. *Arch. Pharm. Res.* **33**, 1665–1670 (2010).
153. Zhu, J. T. T. *et al.* Flavonoids possess neuroprotective effects on cultured pheochromocytoma PC12 cells: A comparison of different flavonoids in activating estrogenic effect and in preventing  $\beta$ -amyloid-induced cell death. *J. Agric. Food Chem.* **55**, 2438–2445 (2007).
154. Feng, Y. *et al.* Resveratrol inhibits beta-amyloid oligomeric cytotoxicity but does not prevent oligomer formation. *Neurotoxicology* **30**, 986–995 (2009).
155. Ladiwala, A. R. A. *et al.* Resveratrol selectively remodels soluble oligomers and fibrils of amyloid A $\beta$  into off-pathway conformers. *J. Biol. Chem.* **285**, 24228–24237 (2010).
156. Breydo, L. & Uversky, V. N. Structural, morphological, and functional diversity of amyloid oligomers. *FEBS Lett.* **589**, 2640–2648 (2015).
157. Galante, D. *et al.* Differential toxicity, conformation and morphology of typical initial aggregation states of A $\beta$ 1-42 and A $\beta$ py3-42 beta-amyloids. *Int. J. Biochem. Cell Biol.* **44**, 2085–93 (2012).
158. Verdier, Y., Zarándi, M. & Penke, B. Amyloid  $\beta$ -peptide interactions with neuronal and glial cell plasma membrane: binding sites and implications for Alzheimer's disease. *J. Pept. Sci.* **10**, 229–48 (2004).
159. LaFerla, F. M., Green, K. N. & Oddo, S. Intracellular amyloid- $\beta$  in Alzheimer's disease. *Nat. Rev. Neurosci.* **8**, 499–509 (2007).
160. Lacor, P. N. *et al.* Synaptic targeting by Alzheimer's-related amyloid  $\beta$  oligomers. *J. Neurosci.* **24**, 10191–10200 (2004).
161. Haass, C. & Selkoe, D. J. Soluble protein oligomers in neurodegeneration: lessons from the Alzheimer's amyloid  $\beta$ -peptide. *Nat. Rev. Mol. Cell Biol.* **8**, 101–112 (2007).

162. Bamberger, M. E., Harris, M. E., McDonald, D. R., Husemann, J. & Landreth, G. E. A cell surface receptor complex for fibrillar  $\beta$ -amyloid mediates microglial activation. *J. Neurosci.* **23**, 2665–2674 (2003).
163. Tomiyama, T., Kaneko, H., Kataoka, K. I., Asano, S., & Noriaki, E. N. D. O. Rifampicin inhibits the toxicity of pre-aggregated amyloid peptides by binding to peptide fibrils and preventing amyloid-cell interaction. *Biochem. J.* 859–865 (1997). at <<http://www.biochemj.org/content/ppbiochemj/322/3/859.full.pdf>>
164. McLaurin, J., Golomb, R., Jurewicz, A., Antel, J. P. & Fraser, P. E. Inositol stereoisomers stabilize an oligomeric aggregate of alzheimer amyloid  $\beta$  peptide and inhibit A $\beta$ -induced toxicity. *J. Biol. Chem.* **275**, 18495–18502 (2000).
165. Pollack, S. J., Sadler, I. I. J., Hawtin, S. R., Tailor, V. J. & Shearman, M. S. Sulfated glycosaminoglycans and dyes attenuate the neurotoxic effects of  $\beta$ -amyloid in rat PC12 cells. *Neurosci. Lett.* **184**, 113–116 (1995).
166. Davis, J. *et al.* Early-onset and Robust Cerebral Microvascular Accumulation of Amyloid  $\beta$ -Protein in Transgenic Mice Expressing Low Levels of a Vasculotrophic Dutch/Iowa Mutant Form of Amyloid  $\beta$ -Protein Precursor. *J. Biol. Chem.* **279**, 20296–20306 (2004).
167. Miao, J. *et al.* Cerebral microvascular amyloid  $\beta$  protein deposition induces vascular degeneration and neuroinflammation in transgenic mice expressing human vasculotrophic mutant amyloid  $\beta$  precursor protein. *Am. J. Pathol.* **167**, 505–515 (2005).
168. El-Amouri, S. S. *et al.* Neprilysin: an enzyme candidate to slow the progression of Alzheimer's disease. *Am. J. Pathol.* **172**, 1342–54 (2008).

## APPENDIX A: MATLAB CODE

The following code was designed by Nick van der Munnik and was calibrated against manual cell counts.

This script calls the "ghostcells2.m" function which determines cell viability based on an absolute threshold of Caspase pixel intensity (referred to as FITC within the code) averaged within a circle centered around the point of convergence of an identified nuclei.

```
DAPI=[];
FITC=[];
Fig=[];
dataoutput=zeros(numsam,3);
index=zeros(numsam,1);
tic;

i=1;
while i<=9 && i<=numsam
    DAPI=uint8(imread(strcat('DAPI0',num2str(i),'.jpg')));
    FITC=uint8(imread(strcat('FITC0',num2str(i),'.jpg')));
    [dataoutput(i,:),Fig]=ghostcells2(DAPI,FITC);
    index(i,1)=i;
    imwrite(Fig,strcat('MLImage',num2str(i),'.tif'));
    figure
    imshow(Fig)
    i=i+1;
end

while i>9 && i<=numsam
    DAPI=uint8(imread(strcat('DAPI0',num2str(i),'.jpg')));
    FITC=uint8(imread(strcat('FITC0',num2str(i),'.jpg')));
    [dataoutput(i,:),Fig]=ghostcells2(DAPI,FITC);
    index(i,1)=i;
    imwrite(Fig,strcat('MLImage',num2str(i),'.tif'));
    figure
    imshow(Fig)
```

```

    i=i+1;
end
fprintf('average time per sample (minutes)')
toc/(60*numsam)
fprintf(' Index Cells Active_Cells Caspase/Hoeschst)
dataoutput=[index dataoutput]

```

Below is the subroutine ghostcells2.

```

function [data,output]=ghostcells2(D,F)
p=D(:,:,3);      % Uses blue channel for Hoechst
fit=F(:,:,2);    % Uses green channel for Caspase
dim=size(p);
rdim=dim(1,1);
cdim=dim(1,2);

dthresh=5;        % Caspase activation threshold
crad=50;          % Radius of cell

mincon=38;
minex=40;
maxcon=130;
nsteps=5;
pstore=p;
cells=0;
deadcells=0;
q=p*0;
s=p*0;
outputf=p*0;
outputd=p*0;
ltag=p*0;
dtag=p*0;
rtag=p*0;
output=zeros(rdim*2,cdim);
bin=p*0;
negative=p*0;
cidrinit=zeros(1000,1);
cidcinit=zeros(1000,1);

%Count Cells
for step=0:nsteps
    thresh=110-step*(100/nsteps);
    p=pstore;
    %Make Black/White
    for i = 1:rdim
        for j = 1:cdim

```

```

if p(i,j) >= thresh
    p(i,j) = 100;
else
    p(i,j) = 0;
end
if step==nsteps
    if p(i,j) >= thresh
        bin(i,j) = 1;
        negative(i,j)=0;
    else
        bin(i,j) = 0;
        negative(i,j)=100;
    end
end
end
%Outline Cells
for i = 2:rdim-1
    for j = 2:cdim-1
        if p(i,j) ==100
            if p(i-1,j)==0 && p(i+1,j)==100
                p(i,j)=200;
            elseif p(i-1,j)==100 && p(i+1,j)==0
                p(i,j)=200;
            elseif p(i,j-1)==0 && p(i,j+1)==100
                p(i,j)=200;
            elseif p(i,j-1)==100 && p(i,j+1)==0
                p(i,j)=200;
            end
        end
    end
end
p(1,:)=200;
p(:,1)=200;
p(rdim,:)=200;
p(:,cdim)=200;
%Squeeze cell outlines by half minimum feature size
for k=0:(mincon/2)
    for i = 2:rdim-1
        for j = 2:cdim-1
            if p(i,j)==100
                if p(i-1,j)==200+k && p(i+1,j)==100
                    p(i,j)=200+k+1;
                elseif p(i-1,j)==100 && p(i+1,j)==200+k
                    p(i,j)=200+k+1;
                elseif p(i,j-1)==200+k && p(i,j+1)==100

```

```

p(i,j)=200+k+1;
elseif p(i,j-1)==100 && p(i,j+1)==200+k
    p(i,j)=200+k+1;
elseif p(i-1,j)>=200 && p(i+1,j)>=200
    p(i,j)=200+k+1;
elseif p(i,j-1)>=200 && p(i,j+1)>=200
    p(i,j)=200+k+1;
end
end
end
end
for i = 1:rdim
    for j = 1:cdim
        if p(i,j) >= 200
            p(i,j) = 200;
        end
    end
end
for i = 2:rdim-1
    for j = 2:cdim-1
        if p(i,j) ==100
            if p(i-1,j)==200 && p(i+1,j)==200
                p(i,j)=200;
            elseif p(i,j-1)==200 && p(i,j+1)==200
                p(i,j)=200;
            end
        end
    end
end
p=p-q;
for k=0:(maxcon-mincon)/2
    %Test for convergence, exclude area around confirmed cell
    for i = (mincon/2):rdim-(mincon/2)
        for j = (mincon/2):cdim-(mincon/2)
            if p(i,j) ==100
                index=0;
                if p(i-2,j)>=200 && p(i+2,j)>=200
                    if p(i,j-2)>=200 && p(i,j+2)>=200
                        index=1;
                    end
                end
                if p(i-2,j-1)>=200 && p(i+2,j-1)>=200
                    if p(i+1,j-2)>=200 && p(i+1,j+2)>=200
                        index=index+1;
                    end
                end
            end
        end
    end

```

```

end
if p(i-1,j-2)>=200 && p(i-1,j+2)>=200
    if p(i-2,j+1)>=200 && p(i+2,j+1)>=200
        index=index+1;
    end
end
if index==3
    if p(i-2,j-2)>=200 && p(i+2,j-2)>=200
        if p(i-2,j+2)>=200 && p(i+2,j+2)>=200
            cells = cells+1;
            for m = -minex:minex;
                for n = -minex:minex;
                    if sqrt(m^2+n^2)<=minex
                        if i-m>=1 && i-m<=rdim
                            if j-n>=1 && j-n<=cdim
                                q(i-m,j-n)=1000;
                                p(i-m,j-n)=-1000;
                            end
                        end
                    end
                end
            end
        end
        cidrinit(cells)=i;
        cidcinit(cells)=j;
        s(i,j)=1000;
        for m = 0:9;
            for n = 0:9;
                ltag(i-4+m,j-4+n)=1000;
            end
        end
    end
end
end
end
end
end
end
%Continue to Squeeze
for i = 2:rdim-1
    for j = 2:cdim-1
        if p(i,j)==100
            if p(i-1,j)==200+k && p(i+1,j)==100
                p(i,j)=200+k+1;
            elseif p(i-1,j)==100 && p(i+1,j)==200+k
                p(i,j)=200+k+1;
            elseif p(i,j-1)==200+k && p(i,j+1)==100
                p(i,j)=200+k+1;

```

```

elseif p(i,j-1)==100 && p(i,j+1)==200+k
    p(i,j)=200+k+1;
elseif p(i-1,j)==200+(k+1) && p(i+1,j)==200+k
    p(i,j)=200+k+1;
elseif p(i-1,j)==200+k && p(i+1,j)==200+(k+1)
    p(i,j)=200+k+1;
elseif p(i,j-1)==200+(k+1) && p(i,j+1)==200+k
    p(i,j)=200+k+1;
elseif p(i,j-1)==200+k && p(i,j+1)==200+(k+1)
    p(i,j)=200+k+1;
end
end
end
end
end

%Segment Cell Clusters
pc=imcomplement(pstore);
pmin=imimposemin(pc,~bin|s);
p=watershed(pmin);
p=uint8(p);
for i = 1:rdim
    for j = 1:cdim
        if p(i,j) >0
            p(i,j) = 100;
        else
            p(i,j) = 0;
        end
    end
end
outputf=(p/100).*fit;
outputd=(p/100).*pstore;

%Count Caspase Active
cvec=zeros(cells,1);
cidr=cvec;
cidc=cvec;
for i=1:cells
    cidr(i,1)=cidrinit(i,1);
    cidc(i,1)=cidcinit(i,1);
end

for c=1:cells
    i=cidr(c,1);
    j=cidc(c,1);

```

```

fitcsum=uint32(0);
cmoves=0;
for m=-crad:crad
    for n=-crad:crad
        if i+m>1 && i+m<rdim && j+n>1 && j+n<cdim
            if sqrt(m^2+n^2)<=crad
                cmoves=cmoves+1;
                fitcsum=fitcsum+uint32(fit(i+m,j+n));
                if sqrt(m^2+n^2)>crad-1
                    rtag(i+m,j+n)=112;
                end
            end
        end
    end
end
if double(fitcsum/cmoves)>=dthresh
    deadcells=deadcells+1;
    for m = -2:2;
        for n = -2:2;
            dtag(i+m,j+n)=1000;
        end
    end
end
end

outputf=outputf+ltag+rtag-dtag;
outputd=outputd+ltag-dtag;
output=[outputf outputd];
data=zeros(1,3);
data(1,1)=cells;
data(1,2)=caspasecells;
data(1,3)= caspasecells/cells;

```

## APPENDIX B: EXAMPLE OUTPUT FROM MATLAB CODE

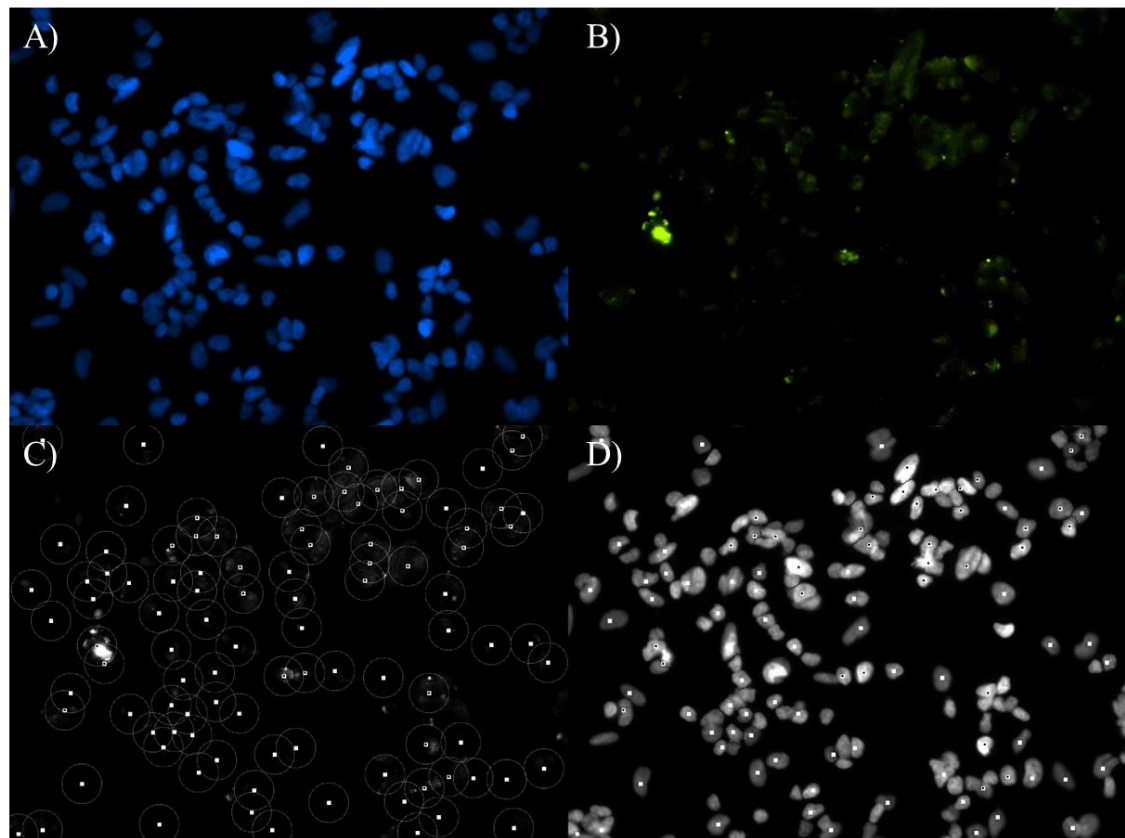


**Figure B.1 Example output from Matlab code.** A) Hoechst image. B) Caspase image. C) Greyscale caspase image. White boxes indicate center of identified nuclei and open circles indicate boundary of cell within which the average pixel intensity from the caspase image was calculated. D) Greyscale of Hoechst image. Nuclei containing both a white and black box were found to have an average caspase pixel intensity above the set threshold and therefore counted as caspase activated cells.

## APPENDIX C: COINCIDING IMAGES FOR FIGURE 3.6

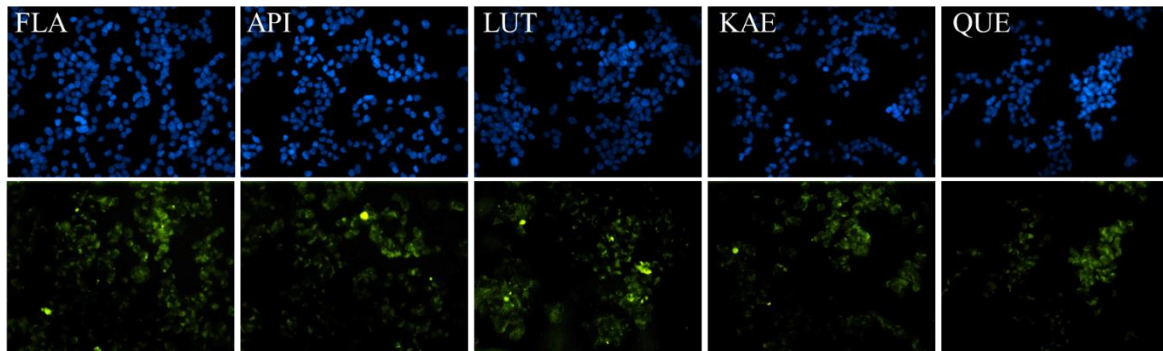


**Figure C.1 Caspase images for cells treated with A $\beta$  oligomers made in the presence of polyphenol.** Hoechst (top panel) and caspase (bottom panel) images that coincide with Figure 3.6 B (open bars).

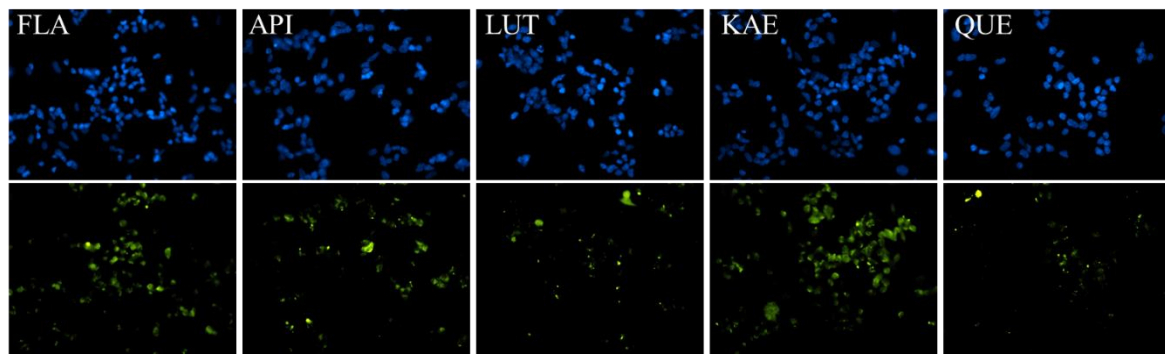


**Figure C.2 Caspase images for cells treated with A $\beta$  oligomers made in the absence of polyphenol and 40  $\mu$ M polyphenol.** Hoechst (top panel) and caspase (bottom panel) images that coincide with Figure 3.6 B (closed bars).

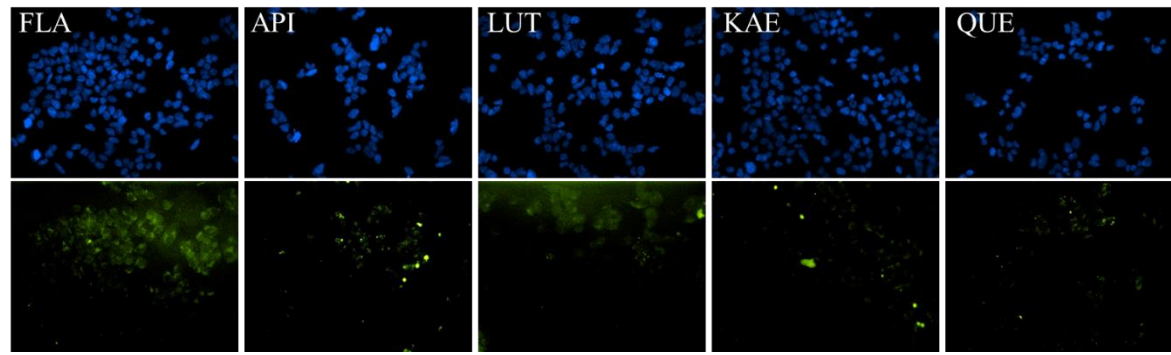


**Figure C.3 Caspase images for dual-action treatment.** Hoechst (top panel) and caspase (bottom panel) images that coincide with Figure 3.6 B (grey bars).

## APPENDIX D: COINCIDING IMAGES FOR FIGURES 4.4 AND 4.5

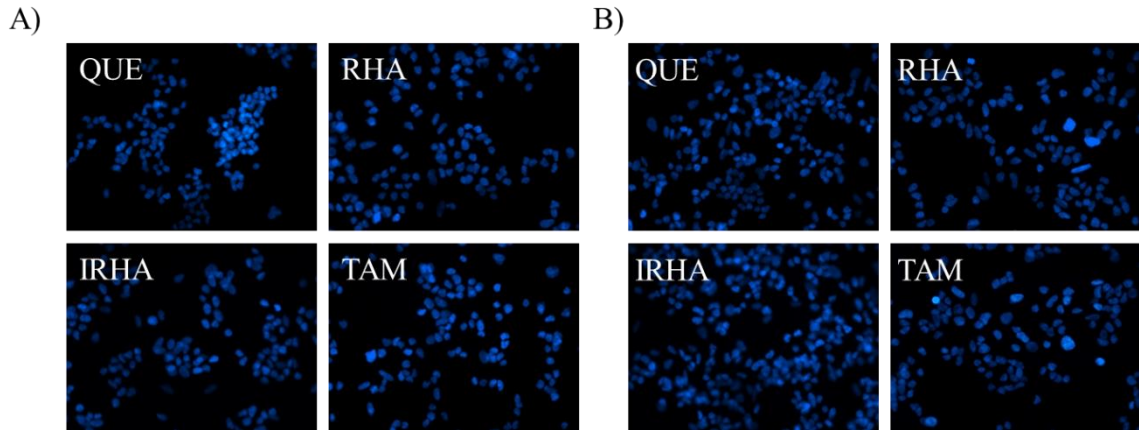


**Figure D.1 Coinciding Hoechst images for Figures 4.4 and 4.5.** Hoechst images for A) cells treated with A $\beta$  oligomers formed in the presence of polyphenol to coincide with Figure 4.5 and B) dual-action treatment to coincide with Figure 4.6.